ARMY RESEARCH LABORATORY

Thermochemical Response of Vinyl-Ester Resin

by Bruce K. Fink, Travis A. Bogetti, Molly A. Stone,
and John W. Gillespie, Jr.

ARL-TR-2653 January 2002

The findings in this report are not to be construed as an official Department of the Army position unless so designated by other authorized documents.

Citation of manufacturer's or trade names does not constitute an official endorsement or approval of the use thereof.

Destroy this report when it is no longer needed. Do not return it to the originator.

Army Research Laboratory
Aberdeen Proving Ground, MD 21005-5069

ARL-TR-2653 **January 2002**

Thermochemical Response of Vinyl-Ester Resin

Bruce K. Fink and Travis A. Bogetti
Weapons and Materials Research Directorate, ARL

Molly A. Stone and John W. Gillespie, Jr.
University of Delaware

Abstract

This report presents the thermochemical characterization of Dow Derakane 411-C50 commercial vinyl-ester resin at low temperatures (20°–40 °C). Differential scanning calorimetry (DSC) and torsional braid analysis (TBA) are the experimental techniques used to characterize the material behavior. The cure kinetics are studied using DSC and are modeled using a modified autocatalytic equation with a maximum degree of cure term. Also, the effect of inhibitors in the resin system is accounted for by an inhibitor depletion model. A time-temperature-transformation diagram is constructed for the material by measuring the times to gelation and vitrification using TBA. The glass transition temperature (T_g) is also characterized using the TBA and related to the degree of cure. It was found that the T_g and the degree of cure do not exhibit a linear relationship for this resin system. The findings presented in this work provide information for accurate cure modeling and process simulation of vinyl-ester materials.

Contents

List of Figures

INTENTIONALLY LEFT BLANK.

List of Tables

INTENTIONALLY LEFT BLANK.

1. Introduction

Vinyl-ester resins are being used extensively as a matrix for liquid-molding composite structures. Vinyl esters exhibit many attractive attributes, including low viscosity (enabling room-temperature infusion into a preform), room-temperature cure, comparable properties with other commonly used resins, and relatively low cost. Unfortunately, however, the thermochemical response of vinyl-ester resins at low temperatures is not well understood.

Knowledge of the cure kinetic behavior of a thermosetting resin is required in establishing appropriate processing strategies that help to ensure satisfactory quality and in-service performance characteristics in the composite. Cure-kinetic behavior involves the many interrelationships that exist between the degree of cure, temperature, time, and various material properties during the cure process. Resin viscosity strongly depends on the degree of cure. During liquid-molding processes, the time to infiltrate must be less than the resin gel time (i.e., the time at which the viscosity approaches infinity) to ensure complete wetting. The glass transition temperature (T_g) of the as-manufactured composite part is governed by the final degree of cure. Process-induced residual stress will also depend on degree of conversion through T_g dependence, as well as the spa concentration, process temperatures, and postcure methods. The complex interrelationship between all of these processing variables demonstrates the need to have a thorough understanding of spatial gradients in cure-dependent modulus and shrinkage that evolve during cure. These parameters can affect initial mold design, resin selection (including inhibitors used to control the cure-kinetic behavior of a thermoset system.

In this work, differential scanning calorimetry (DSC) and torsional braid analysis (TBA) were used to characterize the cure-kinetic behavior of a vinyl-ester resin. Samples cured at low temperatures (i.e., room temperature) do not normally reach conversions as high as those cured at elevated temperatures. The conversion plateaus as the diffusional limitations physically prevent the material from fully reacting. The reaction slows down because the mobility of the unreacted monomer decreases. In this regime, the T_g of the material continues to increase and is very sensitive to slight changes in degree of cure. The slight increase in degree of cure after this point is very difficult to measure using DSC. For the vinyl-ester system, when most of the vinyl ester has already reacted, the styrene conversion continues to increase, yet this corresponds to only a very small amount of reacting material. Since the remaining reaction occurs over a relatively long time and the thermal-generation rate is small, DSC is not sensitive enough to detect the heat being liberated. Therefore, DSC is unable to accurately characterize the cure advance in the late stages of cure when diffusional limitations control the reaction.

TBA was used to study the physical changes occurring in the vinyl-ester resin during cure. The TBA showed that mechanical and chemical changes continue to occur within the resin system long after the maximum degree of cure is achieved. Increases in the resin stiffness (relative rigidity) and the T_g were measured by TBA at times beyond the point at which maximum degree of cure was reached. Also, Fourier transform infrared (FTIR) spectroscopy studies showed the styrene reaction continuing after the vinyl-ester reaction had reached a plateau. During these later stages of cure, the TBA was found to be very sensitive to the mechanical changes in the system, allowing full thermochemical characterization of the system.

In this investigation, both DSC and TBA are used to conduct a comprehensive characterization of the thermochemical behavior of a vinyl-ester resin system during cure. The DSC describes the reaction up to the cure state near the point of maximum conversion. The TBA shows the further increase in T_g and the temperature dependence of the curing mechanisms.

2. Chemistry

2.1 Free-Radical Polymerization

Vinyl-ester resins consist of styrene and a vinyl-ester prepolymer monomer. The chemical structures of these compounds are shown in Figure 1. The vinyl ester provides the important polymer properties such as modulus, T_g, toughness, and durability. The styrene monomer is a reactive diluent. The main purposes of the styrene are to control the viscosity, improve the wetting behavior of the resin, and lower the cost of the overall resin system.

Vinyl esters are synthesized from the reaction of an unsaturated carboxylic acid, such as methyl methacrylate, with an epoxy resin. Vinyl esters differ from unsaturated polyesters in having only carbon-carbon double bonds at the ends of the chain and only pendant hydroxyl groups. The carbon-carbon double-bond end group is known as a vinyl group. Vinyl-ester monomer contains two vinyl end groups that allow a cross-linked structure to form during the reaction, while reaction of the styrene extends the structure in a linear fashion.

These monomers react through a free-radical polymerization. The mechanism of such a reaction is explained by Stevens (1990). For completeness, however, a brief summary of the three main steps of free-radical polymerization is given as follows: (1) initiation involving two reactions—formation of the initiator radical (R) and addition of the initiator radical to a monomer, (2) propagation of a monomer radical to another monomer molecule, and (3) termination of all growing chains due to lack of mobility of unreacted monomers.

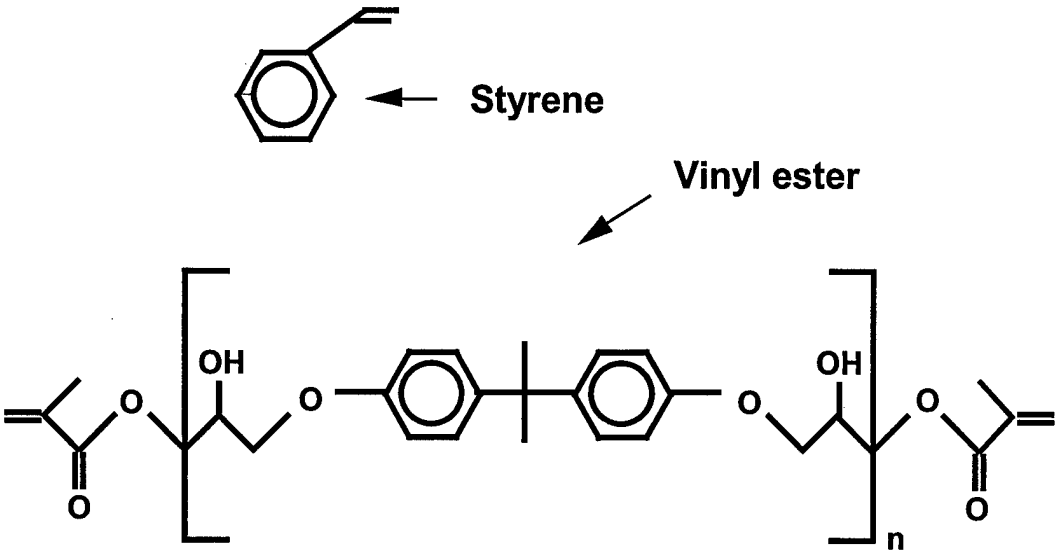

Figure 1. Styrene and vinyl-ester structures.

Possible initiators for a free-radical polymerization include peroxides and hydroperoxides, azo compounds, redox initiators, and photoinitiators (Stevens 1990). The initiator should be relatively stable at room temperature but, to ensure practical reaction rates, should decompose rapidly at polymer processing temperatures. In the current vinyl-ester resin system, an organic hydroperoxide is used as the initiator. Initial radicals are formed through thermal decomposition of the peroxide initiator. The polymerization reaction then propagates through the addition of the monomer to the growing polymer chain and continues propagation of the radical to the new monomer site. The decomposition rate of the initiator can be raised at low temperatures by adding an accelerator or promoter, such as (dimethylamino) benzene, cobalt naphthenate, or dimethyl aniline (DMA).

The vinyl-ester resin used in this investigation is Dow Derakane 411-C50 commercial resin, containing nominally 50 weight-percent styrene. The amount and type of initiator used in the system is 2 weight-percent Trigonox 239 A, produced by Akzo Co. This initiator contains 45% cumyl hydroperoxide, 45% carboxylic ester, and 10% cumyl acid. Cobalt napthenate (CoNap), containing 6% cobalt, was used as an accelerator. CoNap accelerator was added in the amount of 0.2 weight-percent to induce the decomposition of the initiator at low curing temperatures. An inhibitor, 4-methoxyphenol, was added to the system in the amount of 0.3 weight-percent. The purpose of the inhibitor, as well as its effect on the cure reaction, is discussed next. Also present in the commercial vinyl-ester resin is an inhibitor to lengthen the shelf life. The type of inhibitor was not reported by Dow, nor was the nature of the carboxylic ester in the Trigonox 239 A reported by Akzo.

2.2 Effect of Added Inhibitor on the Reaction Behavior

During initial curing experiments at room temperature, DSC thermograms showed that reaction of the vinyl-ester resin began almost immediately after the CoNap accelerator and Trigonox initiator were added. This phenomena caused concern both from a processing and an experimental point of view. Because of the desire to better control and observe the start of the reaction, 4-methoxyphenol inhibitor was added to the system to delay the cure.

Adding 0.3% 4-methoxyphenol delayed the start of the vinyl-ester reaction at cure temperatures between 20° and 40 °C. However, the reaction rate was found to increase after the inhibitor was added, as shown in Figure 2. The same results were found when a retardant, 2,4-pentadione, was added to the system. Separate studies were conducted by Ziaee and Palmese (1999), where an unknown inhibitor added by Dow was removed, leaving only vinyl ester and styrene. Comparisons between these rates of reaction showed that the reaction rate was decreased by removing the inhibitor. This result is consistent with the findings of the 2,4-pentadione and 4-methoxyphenol additions. It is concluded then that when adding an inhibitor or retardant to the vinyl-ester system, which is commonly done in processing, it should not be presumed that the rate of reaction will be unaffected. These results also imply that caution is necessary when changing the resin composition.

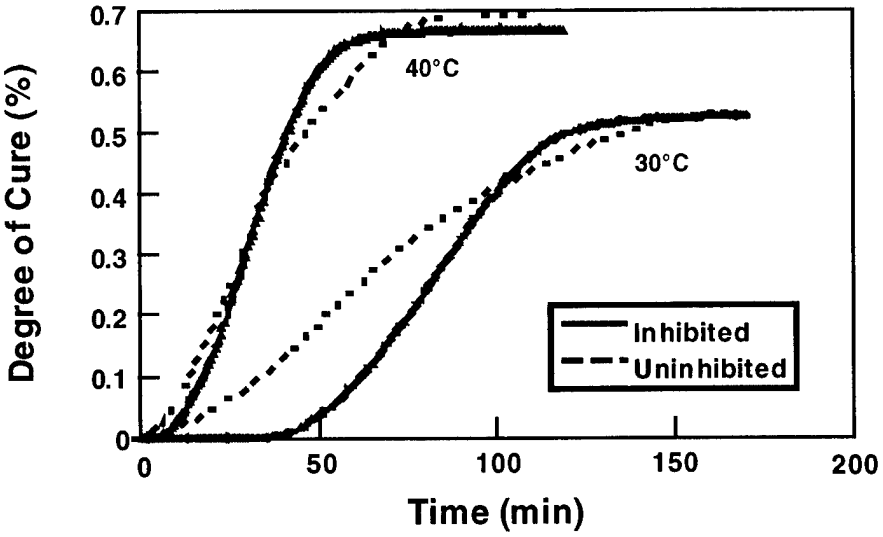

Figure 2. The effect of 4-methoxyphenol inhibitor on the degree of cure.

3. Theory

3.1 Degree of Cure Calculation

A common method of defining the extent of chemical conversion is by directly relating the heat of reaction to the degree of cure. For isothermal curing, it is assumed that the heat generated at different times during the reaction is directly proportional to the degree of cure. DSC is widely accepted as an accurate technique to measure the heat of reaction during cure and thus to determine the degree of conversion.

The heat generated by a reaction at any time, t, is given by

$$\Delta H = \int_0^t \left(\frac{dQ}{dt} \right) dt, \tag{1}$$

where dQ/dt is the rate of heat generation. Each resin system has an ultimate heat of reaction, ΔH_{ult}, which would be given off if the reaction were to fully reach completion. For a particular resin system, ΔH_{ult} can be found by curing the system using a slow-temperature ramp and measuring the total heat of reaction. This value cannot normally be reached during a typical isothermal cure and is not often reached, even after a postramp experiment. At the completion of an isothermal cure, the total heat released is given by ΔH_{iso}. A subsequent temperature ramp will yield a residual heat of reaction, ΔH_{resid}. Theoretically, the sum of ΔH_{iso} and ΔH_{resid} would equal ΔH_{ult}. Experimentally, however, this is not always the case. Also, the sum of ΔH_{iso} and ΔH_{resid} is not constant for various cure temperatures. Reasons for these phenomena may include a change in the curing mechanism that depends on the cure history or physical restrictions of the material that do not allow the full heat to be generated. In either case, it would not be accurate to use the sum of the isothermal and residual heats of reaction as the basis for 100% cure. In this work, full cure is based on the ultimate heat of reaction, ΔH_{ult}, measured from the DSC experimental temperature ramps.

Therefore, the method chosen for calculating the degree of cure at any time is based on the following equation:

$$\alpha(t) = \frac{\Delta H(t)}{\Delta H_{ult}}. \tag{2}$$

This equation states that the degree of cure at any time, $\alpha(t)$, is determined by the percentage of the total available heat of reaction that has been released. Also, the rate of cure is proportional to the rate of heat being released, dQ/dt, at an isothermal temperature, T_I, and is given by

$$\frac{d\alpha}{dt} = \frac{1}{\Delta H_{ult}} \left(\frac{dQ}{dt} \right)_{T_i} . \tag{3}$$

As mentioned previously, 100% conversion is not often reached during an isothermal cure, especially at low cure temperatures such as those studied in this investigation. Therefore, equation 2 can never reach unity, and a maximum degree of cure, α_{max}, is realized that is less than unity.

The maximum degree of cure is given by the following equation:

$$\alpha_{max} = \frac{\Delta H_{iso}}{\Delta H_{ult}} . \tag{4}$$

The heat of reaction at the end of an isothermal experiment, ΔH_{iso}, will increase as the cure temperature increases; therefore, the maximum degree of cure will also increase. Experiments have shown that the maximum degree of cure increases linearly with an increase in isothermal cure temperature (Michaud 1996). A function describing $\alpha_{max}(T)$ can then be extrapolated to nearby temperatures.

3.2 Kinetic Modeling

When the exact reaction mechanism is not known, models based on empirical rate laws are frequently used to describe the rate of cure. Depending on the type of reaction, various kinetic models have been used to approximate the curing process of thermosetting resins.

The autocatalytic model has been widely used to describe the kinetics of some epoxy resins and, more recently, has been found to fit the cure behavior of vinyl-ester resins. The autocatalytic equation allows for an induction period before the reaction, which is typical of many thermosets. An autocatalytic reaction is defined as a reaction in which one of the products of the reaction acts as a catalyst (Levenspiel 1972). A product must be present if the reaction is to proceed at all. At the beginning of the reaction, a very small concentration of product usually exists, and the reaction rate is low. As more product is formed, the reaction rate rises to a maximum. Finally, the rate decreases as the reactant is consumed. The following autocatalytic model was suggested by Kamal and Sourour (1973) and is recommended by other workers to describe the rate of cure for certain thermosetting resins (Dillman and Seferis 1987; Han and Lem 1983; Hong and Chung 1991; Lee and Lee 1994; Michaud 1996; Yi et al. 1995), as in

$$\frac{d\alpha}{dt} = \left(k_1 + k_2 \alpha^m \right) \cdot (1 - \alpha)^n . \tag{5}$$

In equation 5, k_1 and k_2 are reaction rate terms, and m and n are exponential constants. Han and Lem (1983) have found k_1 and k_2 experimentally for a vinyl-ester resin system while assuming a second-order reaction, $m + n = 2$. The

reaction-rate terms in equation 5 are assumed to follow an Arrhenius temperature dependency such that

$$ln\, k_1 = ln\, A_1 - \left(E_{a1} / RT\right) \text{ and } ln\, k_2 = ln\, A_2 - \left(E_{a2} / RT\right), \tag{6}$$

where A_1 and A_2 are pre-exponential coefficients, E_{a1} and E_{a2} are activation energies, and R and T are the universal gas constant and temperature, respectively. It has often been found that the k_1 term in equation 5 can be neglected. However, for the vinyl-ester resin system used in this investigation, the k_1 term was found to be important in maintaining numerical stability of the solution technique due to cure rate changes occurring early in the reaction. This point is explained in further detail by Stone (1997). Based on the findings presented by Michaud (1996) for a similar vinyl-ester resin system, the exponential constants m and n were assumed to be constant and independent of temperature.

The activation energy of a reaction can be determined by measuring the times to specific conversions for various cure temperatures. This method is often used with the autocatalytic model by assuming that the reaction-rate terms follow an Arrhenius temperature distribution, as shown in equation 6. A nonlinear regression technique is used to fit the experimental rate data to the kinetic model. A logarithmic plot of the rate term, k_1, vs. the inverse cure temperature gives a straight line with a slope equal to the activation energy, E_{a1}, and an intercept value equal to the pre-exponential parameter, A_1. In this investigation, the autocatalytic model had to be modified to fit the vinyl-ester resin system. In equation 5, the numerical constant *1* is replaced with an α_{max} term to capture the change in maximum conversion with the cure temperature. The following rate equation is therefore used in this work:

$$\frac{d\alpha}{dt} = \left(k_1 + k_2\alpha^m\right)\cdot\left(\alpha_{max} - \alpha\right)^n, \tag{7}$$

where the temperature dependence on α_{max} is discussed in a subsequent section.

3.3 Time-Temperature-Transformation (TTT) Diagram

The TTT diagram is a useful method for displaying the various phase transitions that a thermoset material experiences during cure (Gillham and Enns 1994). The relationships between material transitions and material properties can be easily shown. The TTT diagram is constructed by plotting the time to reach a material transition for each isothermal temperature. A typical TTT diagram for a well-behaved epoxy system is shown in Figure 3.

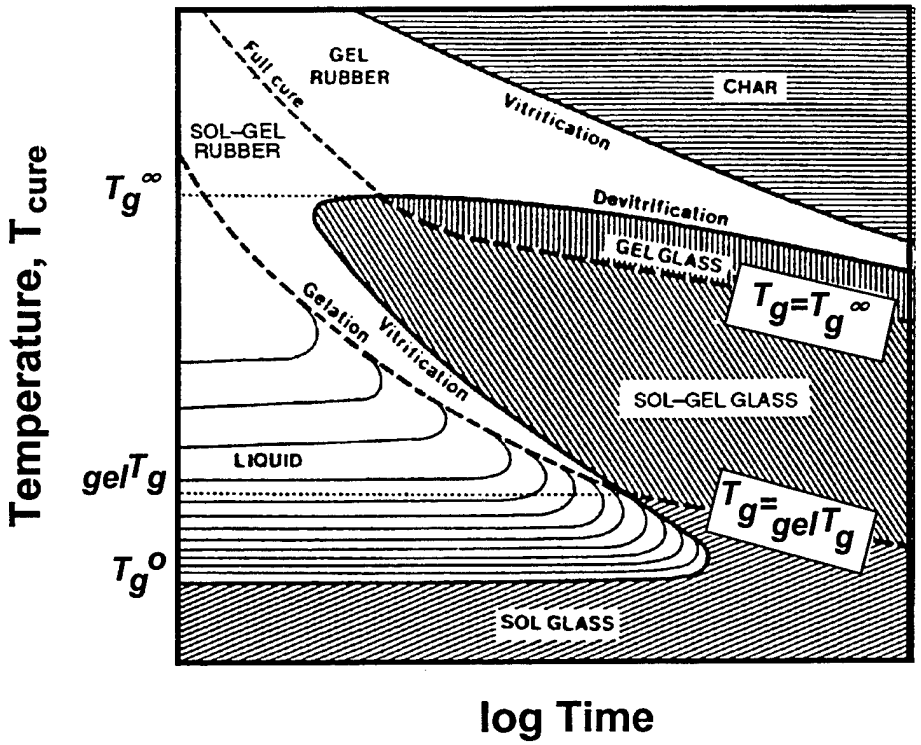

Figure 3. Typical TTT diagram for a well-behaved epoxy system (Gillham and Enns 1994).

During a cure reaction, there are four main physical states that the thermoset material may experience: (1) liquid, (2) ungelled (sol) glass, (3) gelled rubber, and (4) gelled glass. These material phases, as well as transition times, are conveniently identified in the TTT diagram. Three temperatures are important to notice in the TTT diagram: (1) the initial T_g, (T_g^o); (2) the final T_g, (T_g^∞), and (3) the point where the gelation and vitrification times occur simultaneously ($_{gel}T_g$). A curve can be drawn starting at T_g^o, connecting all the vitrification points and ending at T_g^∞. This curve typically exhibits an s-shape. Lines representing the times to gelation and other isoconversion lines can be added. By identifying where the isothermal cure temperature (T_{cure}) occurs in relation to the three characteristic T_g's, important information on the state of the final material can be concluded.

4. Experimental Procedure

A DuPont 700 DSC was used to analyze the kinetic behavior of the material. When characterizing the vinyl-ester resin, isothermal DSC runs at temperatures of 20°, 30°, and 40 °C were conducted. A liquid-nitrogen purge was maintained

during the experiment, and hermetically sealed pans were used. A weight of more than 1.0% was not accepted. The heat flow was then measured to allow for calculating the degree and rate of cure. An Arrhenius temperature dependency was assumed for the rate constant, thus providing the parameters necessary to model the cure kinetics.

A TBA was used to characterize the time-temperature dependence of the T_g and rigidity associated with the cure and to measure the times to specific material transitions. TBA is a dynamic mechanical technique capable of capturing the material behavior through the liquid, rubbery, and glassy stages of cure. The TBA sample consists of a glass braid substrate saturated with liquid resin. As the material cures, torsional oscillations are applied and the change in the damping response of the braid is measured. The anisotropy of the braid allows the torsional rigidity to be dominated by the resin. The temperature was carefully controlled during the experiment, and a liquid-nitrogen purge was used. The times to gelation and vitrification were measured during isothermal cures, as well as the increasing rigidity. The increase in T_g during cure was tracked by quenching the specimen at various stages in the cure and increasing the temperature through the T_g.

5. Results and Discussion

5.1 DSC Results

5.1.1 Degree of Cure Calculation

In Figure 4, the area under the isothermal curve was calculated at each time increment, and the instantaneous degree of cure was calculated from equation 2. A value of 420 J/g for ΔH_{ult} was experimentally determined by ramping the system from room temperature to 250 °C at 5 °C/min. A similar ΔH_{ult} value of 425 J/g was determined by Palmese et al. (1998). Typical experimental degree of cure vs. time curves for various isothermal temperatures are shown in Figure 5. The resin conversion increases with increasing cure temperature, and the total cure time decreases. The effect of the added inhibitor can be seen by the time it takes for the reaction to begin. It is evident that inhibitor effectiveness is greater for lower cure temperatures.

Table 1 shows the DSC results from the three isothermal conditions with equation 4 used to calculate α_{max}. Ideally, the sum of the isothermal and residual heats of reaction would give the achievable heat of reaction for the system. However, it can be seen from Table 1 that this is not the case. The low heat of reaction generated during the isothermal cure is due to increased

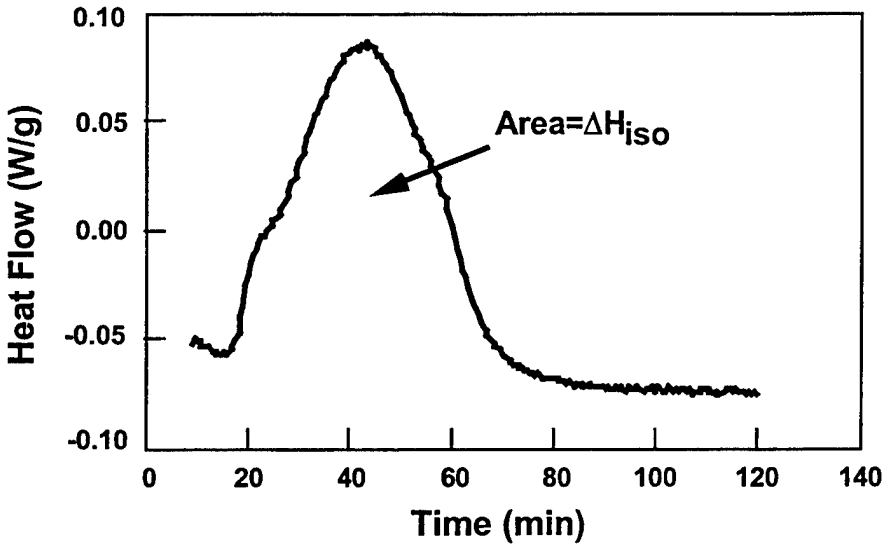

Figure 4. DSC thermogram from an isothermal experiment at 40 °C.

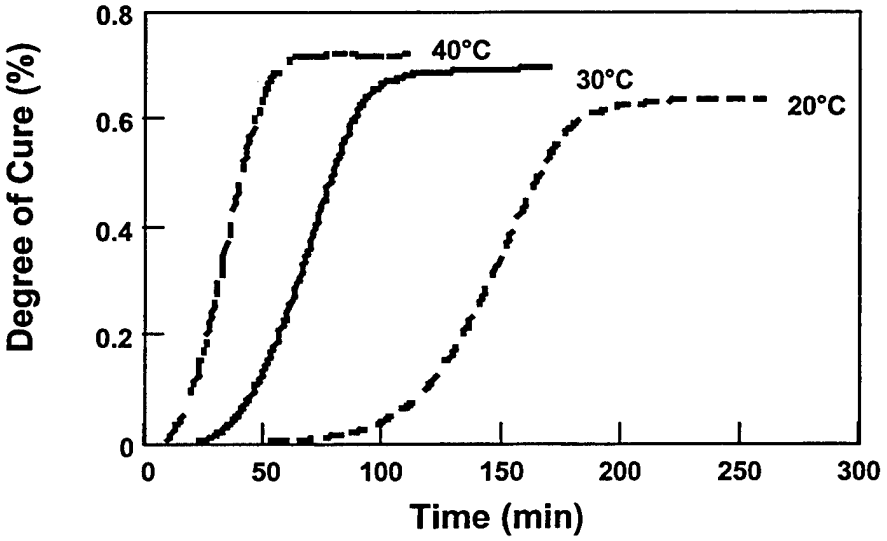

Figure 5. Experimental isothermal degree of cure profiles for vinyl-ester resin cured at 20°, 30°, and 40 °C.

diffusional limitations at lower cure temperatures. This results in a maximum degree of cure of less than one. The maximum degree of cure is expressed as a linear function of temperature in equation 8,

$$\alpha_{max}(T) = 0.53407 + (0.0044572)T(°C). \quad (8)$$

Table 1. Vinyl-ester DSC results from 20°, 30°, and 40 °C isothermal cures.

Temp. (°C)	ΔH_{iso} (J/g)	ΔH_{resid} (J/g)	ΔH_{total} (J/g)	α_{max}
20	261.2 ± 7.7	100.1 ± 1.8	361.3 ± 6.2	0.6217 ± 0.0187
30	281.6 ± 12.7	85.0 ± 4.4	366.6 ± 17.3	0.6705 ± 0.0307
40	278.6 ± 3.8	58.5 ± 2.3	357.1 ± 1.6	0.7110 ± 0.0072

At lower temperatures, therefore, a lower α_{max} is expected, as shown in Figure 6. The residual heats of reaction were found to decrease as the isothermal temperature increased. This is in agreement with other reports showing the residual heat to be a linearly dependent function of temperature, decreasing with increasing temperature (Lee and Han 1987). This behavior appears to be reasonable since the degree of cure generally increases with increasing temperature.

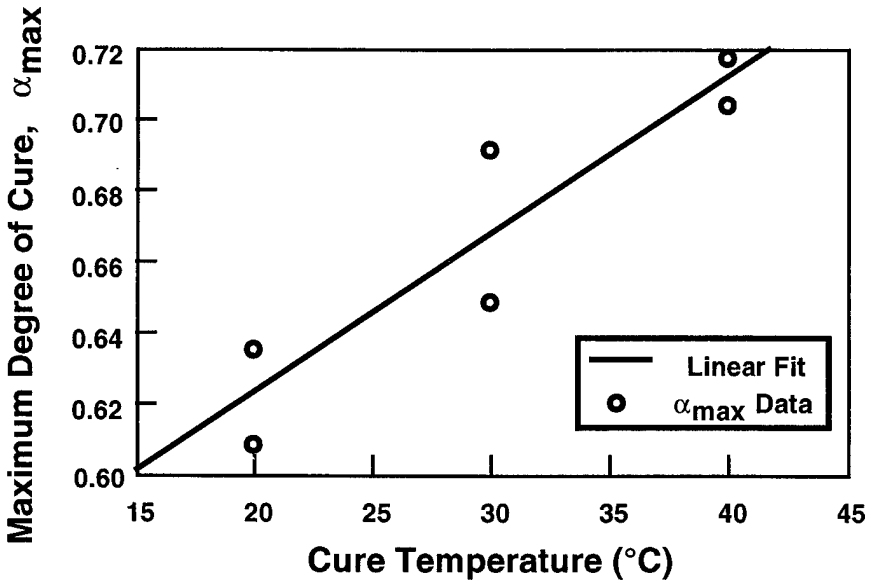

Figure 6. Linear fit of the maximum degree of cure as a function of cure temperature.

5.1.2 Kinetic Parameters

A nonlinear regression technique was used to fit the cure rate curves to equation 7. A second-order reaction ($m + n = 2$) is typically assumed for thermosets. Figure 7 shows the experimental fit of the rate of change of the degree of cure to the second-order autocatalytic model for 20°, 30°, and 40 °C cures. The reaction rates appear to follow the autocatalytic shape, except at the two shoulders, where unusual rate changes were observed. Figure 7 also shows that the model overstates the maximum cure rate by as much as 7.2%.

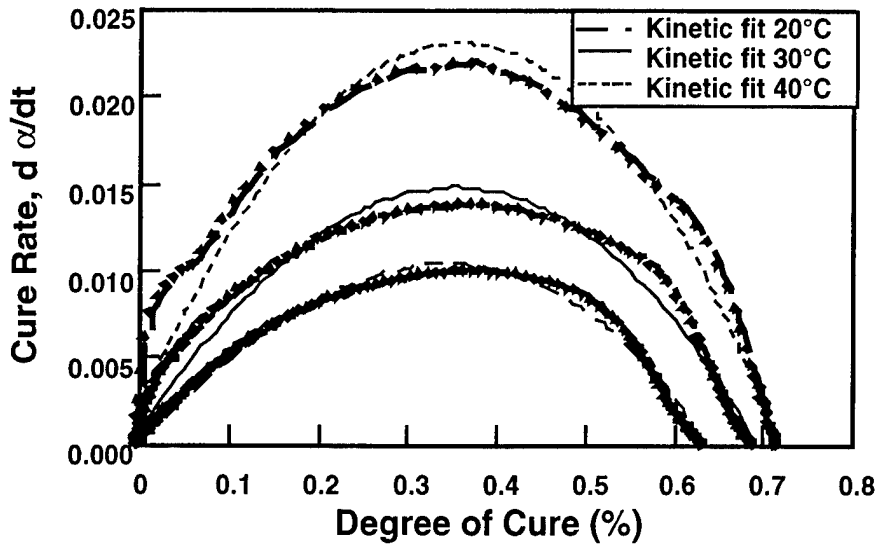

Figure 7. Experimental data showing the rate of cure vs. the degree of cure for a 40 °C isothermal cure (second-order autocatalytic model).

Reactions with orders other than second order were investigated in an attempt to improve model correlation with the data. A fit was conducted with both *m* and *n* as independent parameters. The result of this exercise is shown in Figure 8 for the 40 °C isothermal cure. This model did not provide a significant improvement in the match to the experimental; consequently, the second-order model was used in this work.

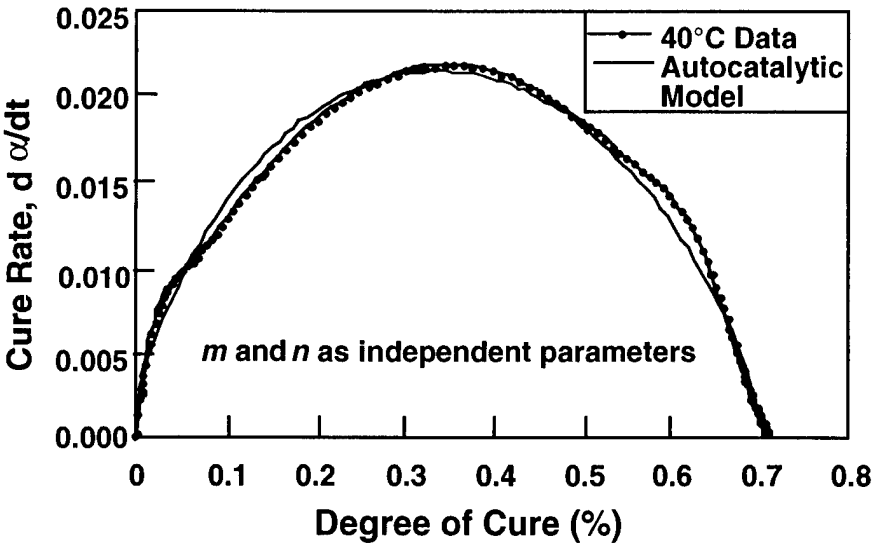

Figure 8. Experimental data showing the rate of cure vs. the degree of cure for a 40 °C isothermal cure (*m* and *n* as independent parameters).

The four kinetic parameters in the second-order autocatalytic model, k_1, k_2, m, and n were determined from the data at each isothermal temperature. The resulting kinetic parameters are given in Table 2. Correlation coefficients indicate that using the autocatalytic model is acceptable for determining the kinetic parameters. However, as can be seen in Figure 7, the presence of the additional shoulders hinder a more exact fit.

Table 2. Kinetic parameters in the second-order autocatalytic model.

Temp. (°C)	k_1 (1/min)	k_2 (1/min)	m	n	Corr. Coeff.
20	0.00031 ± 0.00010	0.07771 ± 0.00200	1.075 ± 0.015	0.725 ± 0.015	0.7747
30	0.00117 ± 0.00001	0.12733 ± 0.00700	1.038 ± 0.004	0.762 ± 0.004	0.7700
40	0.00348 ± 0.00007	0.16737 ± 0.00200	1.037 ± 0.007	0.763 ± 0.007	0.7875

The average values of k_1 and k_2 for each isothermal cure were used to generate an Arrhenius plot, as shown in Figure 9. Linear equations for the rate constants are given in equations 9 and 10. The pre-exponential factors and activation energies were determined from the y-intercepts and slopes of the linear equations and are given in Table 3.

$$\ln k_1 = 2.0808 - 20{,}719(1/RT_{cure}). \tag{9}$$

$$\ln k_2 = 27.173 - 96{,}346(1/RT_{cure}). \tag{10}$$

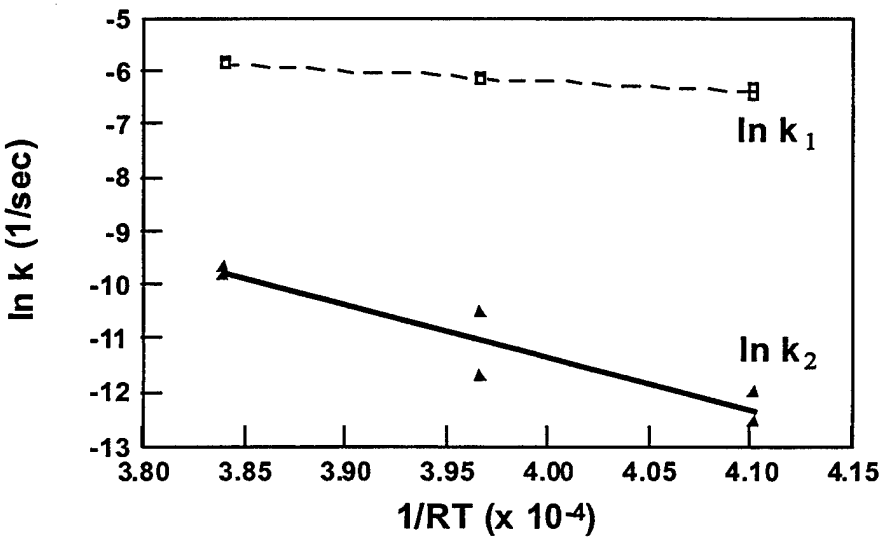

Figure 9. Arrhenius plot of the rate constants for the autocatalytic equation.

Table 3. Arrhenius parameters for the rate constants in the second-order autocatalytic model.

	E_a (J/mol)	A (1/min)
k_1	20,719	4.80×10^2
k_2	96,346	3.80×10^{13}

The kinetic model just presented represents the cure behavior of the resin. In addition to the kinetic model, the delay in cure caused by the reaction inhibitors represents another important aspect for consideration to accurately model the vinyl-ester cure. Inhibitors are present in the resin upon shipping, and an additional inhibitor was added to the resin in this investigation. These inhibitors need to be depleted by the system before any reaction can begin. This time lapse is not accounted for in the cure-kinetic model just developed. Figure 5 showed that the length of time it takes for the reaction to begin does not change linearly with cure temperature. In fact, it was found to increase exponentially with decreasing cure temperature and can therefore be expressed using an Arrhenius temperature dependency. The complete description of cure is made by modeling the inhibitor depletion first, and then the general kinetic model.

Arrhenius parameters to describe the rate of depletion of the inhibitor can be determined by plotting the inverse of the time for the reaction to start (t_{lag}) against the inverse cure temperature ($1/T_{cure}$). This Arrhenius plot is shown in Figure 10, and equation 11 provides the corresponding linear equation. The parameters for the lag time (depletion) model are given in Table 4.

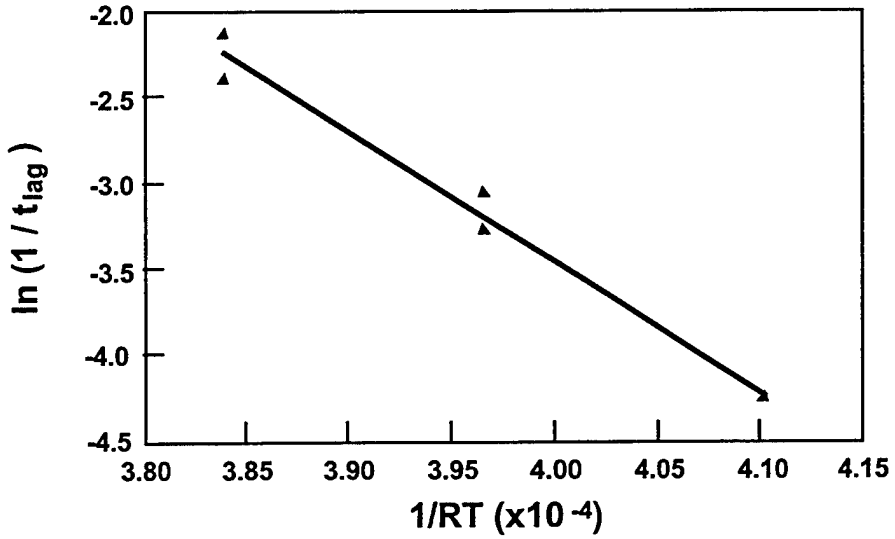

Figure 10. Arrhenius plot showing the change in time for inhibitor depletion with cure temperature.

$$ln(1/t_{lag}) = 26.093 - 83{,}052(1/RT_{cure}). \quad (11)$$

Table 4. Arrhenius parameters for the lag-time model.

	E_a (J/mol)	A (1/min)
k	83,052	1.2884×10^{13}

When the two models (lag-time and cure-kinetic model) are combined, they can accurately predict the total reaction behavior of the resin, starting with the depletion of the inhibitor and continuing with the kinetic reaction. Figure 11 shows how the two models combine. First, the lag-time model demonstrates the rate of depletion of the inhibitor, after which the kinetic model takes over with a description of the cure reaction.

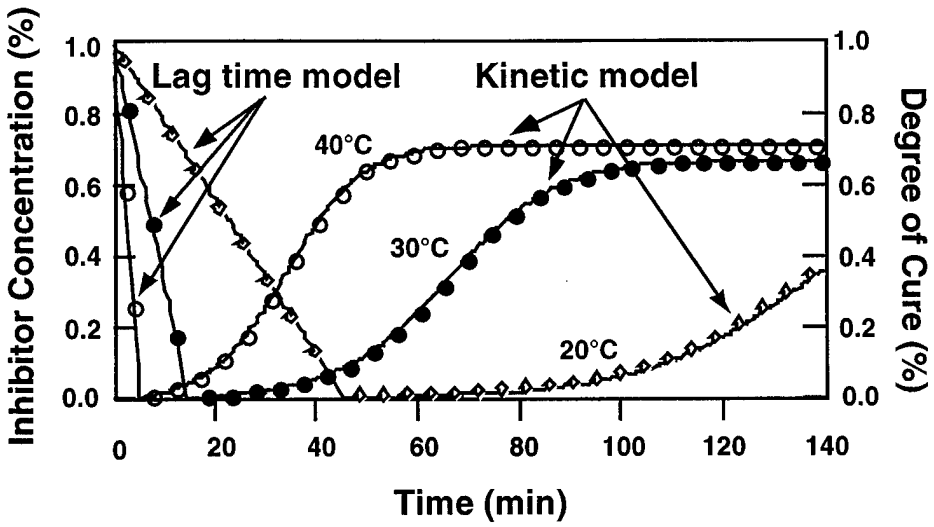

Figure 11. Lag-time model combined with the kinetic model. After the inhibitor concentration reaches zero, the cure-kinetic model begins.

5.1.3 Degree of Cure Correlation

The comparison of the cure simulation models and the experimental degree of cure data is shown in Figure 12. As shown, the inhibitor depletion model worked well to predict the amount of time that would elapse before the reaction progressed. As predicted, this behavior is not linear with temperature, but follows an Arrhenius temperature dependency. The fit is very good, showing that the combination of the kinetic model and inhibitor depletion model is capable of predicting the degree of cure at any time for cure temperatures

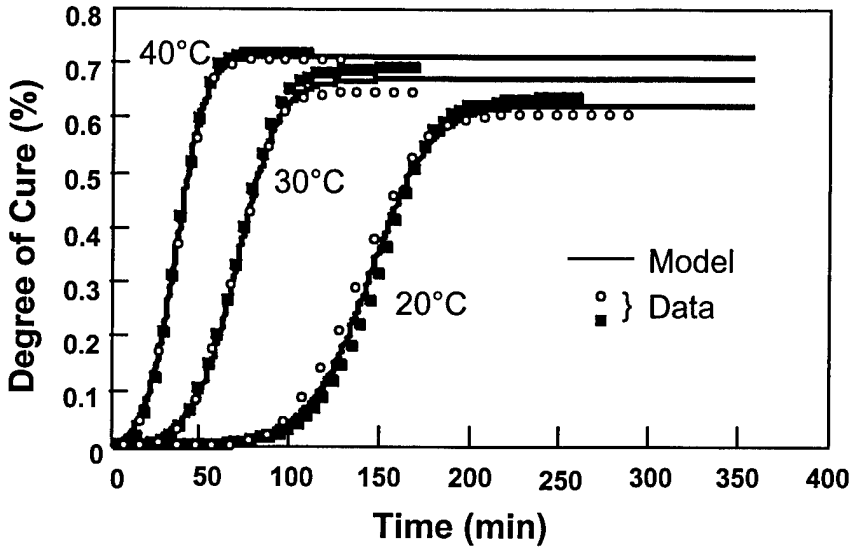

Figure 12. Fit of kinetic model to isothermal DSC data at 20°, 30°, and 40 °C.

between the experimental temperatures of 20°, 30°, and 40 °C. Also, it can be assumed that predictions will be accurate for temperatures within the temperature range that was characterized.

5.1.4 Unusual Vinyl-Ester Resin Behavior

Through the DSC testing, unusual curing behaviors were identified in the vinyl-ester resin system. These behaviors can be explained in part by the interactions of separate chemical reactions and by the effects of a low curing temperature. During the reaction of the vinyl-ester resin system, competing reactions are taking place, specifically vinyl-ester addition to styrene and styrene addition to vinyl ester. The following interesting behaviors have been noticed.

5.1.4.1 Microgel Formations

As the vinyl-ester resin reacts, small clusters of vinyl ester, called microgels, may form. A gel is formed when the polymer swells in the presence of solvents. Microgels are small gel particles between 300 and 1000 μm and are tightly packed spheres that can be suspended in solvents (Stevens 1990). Vinyl-ester microgels form when the styrene solvent swells the polymer. The groups of microgels have some styrene monomers inside of them, but the majority of the remaining styrene monomers are in the surrounding areas. These microgels affect the diffusion of the monomers. Brill et al. (1996) have captured the microgel formation in a similar vinyl-ester resin cured at 70 °C using atomic force microscopy (AFM). This micrograph is shown in Figure 13.

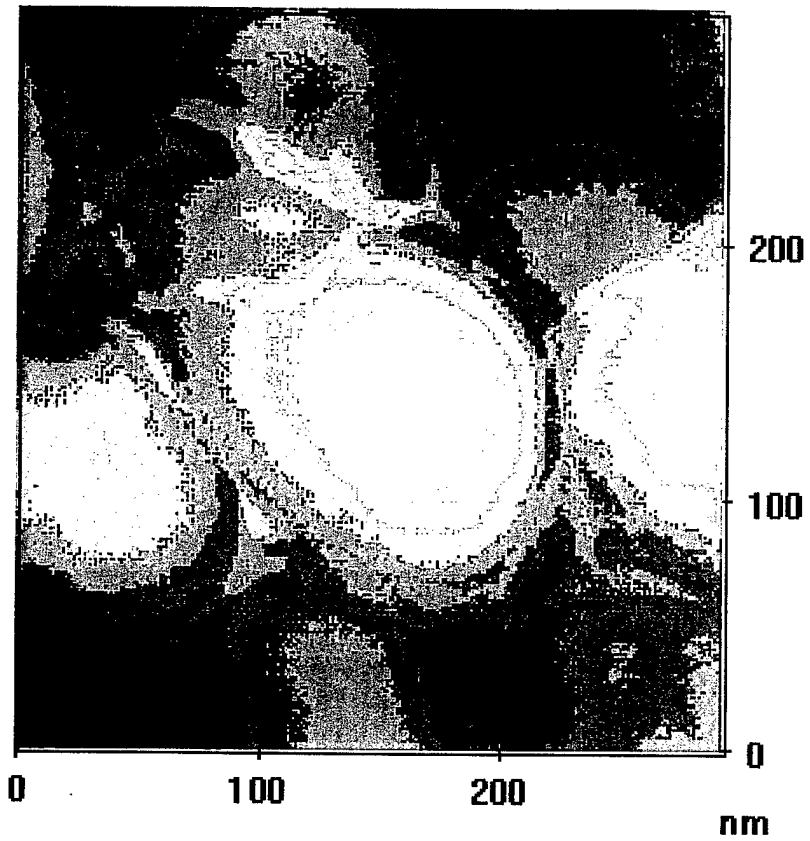

Figure 13. AFM micrograph showing the microgel formation early in the curing process for a vinyl ester, 70 °C isothermal cure (Brill et al. 1996).

5.1.4.2 Diffusional Limitations

In Figure 4, a large exotherm and two plateaus were observed during the isothermal cure. The two plateaus show a sudden decrease in the reaction rate. This is unusual in a thermosetting cure, where typically the reaction rate increases to a maximum and then steadily decreases. Through the use of FTIR spectrometry, Ziaee and Palmese (1999) have shown that at low temperatures, the reaction rate of the vinyl ester is higher than the reaction rate of the styrene monomers in the initial stages of cure. Thus, in the beginning of the cure, the vinyl ester dominates the reaction; this means that for every styrene monomer attaching to the main chain, there is more than one vinyl-ester monomer attaching. The first shoulder is believed to be due to diffusion phenomena. At some point after the initial microgel structure has formed, the vinyl-ester microgels collapse, or tighten around themselves. This reduces the mobility of the vinyl-ester monomers, making it more difficult for them to reach free chain radicals. In addition, the styrene monomers are more restricted from reaching the free radicals in the microgel because of the difficulty they have in diffusing through the now tight microgel structure. This is believed to be the cause of the

sudden, temporary decrease in reaction rate. Once this microgel collapse has occurred, the reaction rate again begins to increase to its maximum rate. FTIR has also shown that when the vinyl-ester reaction rate reaches its maximum, the styrene reaction rate is still increasing (Brill et al. 1996; Ziaee and Palmese 1999). The FTIR results from Brill et al. are shown in Figure 14 for a similar vinyl-ester resin cured at 70 °C. The styrene continues to react long after the leveling off of the DSC thermogram occurs. The styrene monomers are very small and have fewer steric hindrances, which allows them to continue to reach reactive sites long after the vinyl-ester reaction has terminated. As the cure temperature is decreased, the differences in reaction rates become less distinct, and the curve more closely resembles a typical autocatalytic shape.

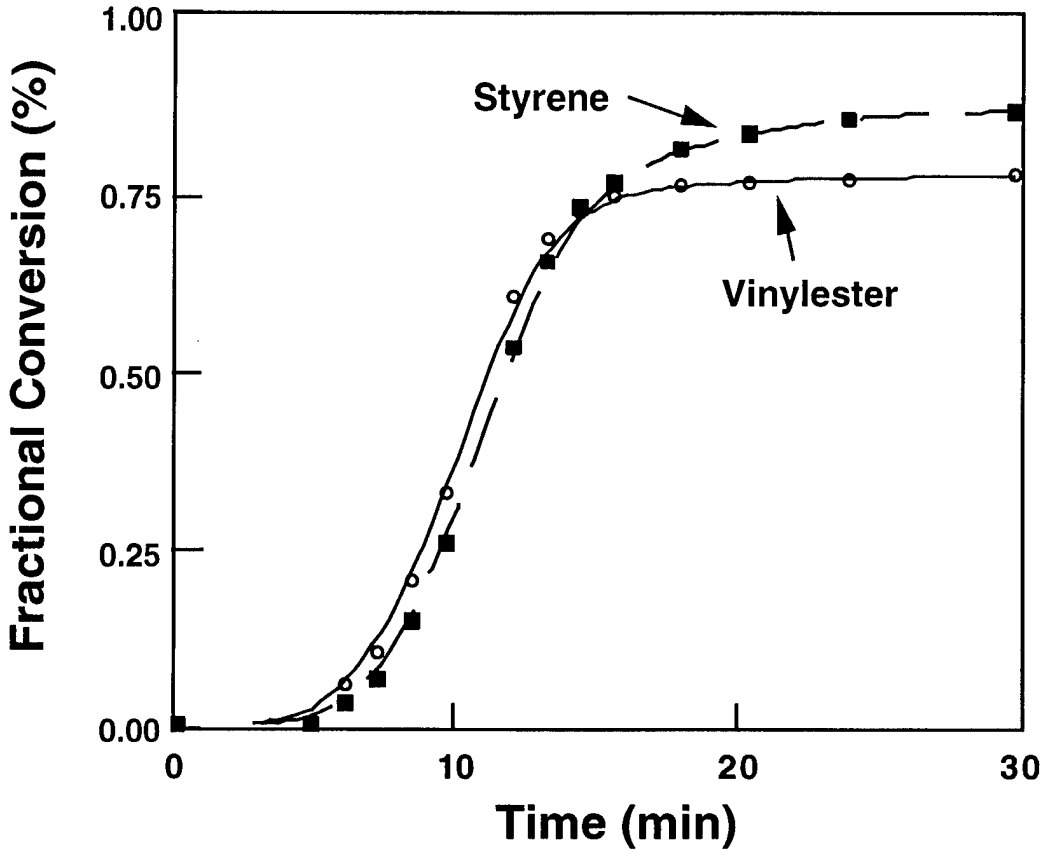

Figure 14. Relative rates of reaction of the vinyl-ester and styrene reactions for a 70 °C isothermal cure (as determined by FTIR spectroscopy) (Brill et al. 1996).

5.1.4.3 Low Maximum Degree of Cure

For any system, a maximum degree of cure, α_{max}, is reached when diffusional limitations hinder the ability of the material to react. The low maximum degree of cure for the vinyl-ester system is due to the diffusional limitation being

reached at a lower conversion compared to that of high-temperature cures. This happens because the molecules have a low thermal energy to begin with. The maximum degree of cure is defined as the maximum conversion that can be detected by the DSC. This occurs soon after the material vitrifies or solidifies. Over an extended period of time, however, the degree of cure may slowly increase beyond α_{max}. This is because the small styrene monomers are still able to diffuse through the solid material to find reactive sites.

5.2 TBA Results

5.2.1 Typical TBA Isotherm and Ramp

Figure 15 shows the typical response observed from a TBA experiment for the isothermal cure (40 °C) of a glass braid specimen impregnated with vinyl-ester resin. Two log relationships are shown—Log(LogD) and Log(rigidity) vs. Log(time). The LogD relationship shows a maximum at material transitions and is calculated by measuring the decay of the successive peak amplitudes as the specimen responds to an applied torsional oscillation. The first peak in the LogD curve is identified as the molecular gelation or a liquid to rubber transition. The second, more prominent peak is identified as the vitrification. The vitrification peak corresponds with the maximum rate of change of the rigidity. The vitrification peak was found to occur earlier than the leveling-off point in the DSC thermogram, which is often taken as the vitrification. This occurrence is discussed further. The rigidity can be seen to continue to increase long after the vitrification peak has occurred and also long after the degree of cure has reached its maximum from DSC measurements.

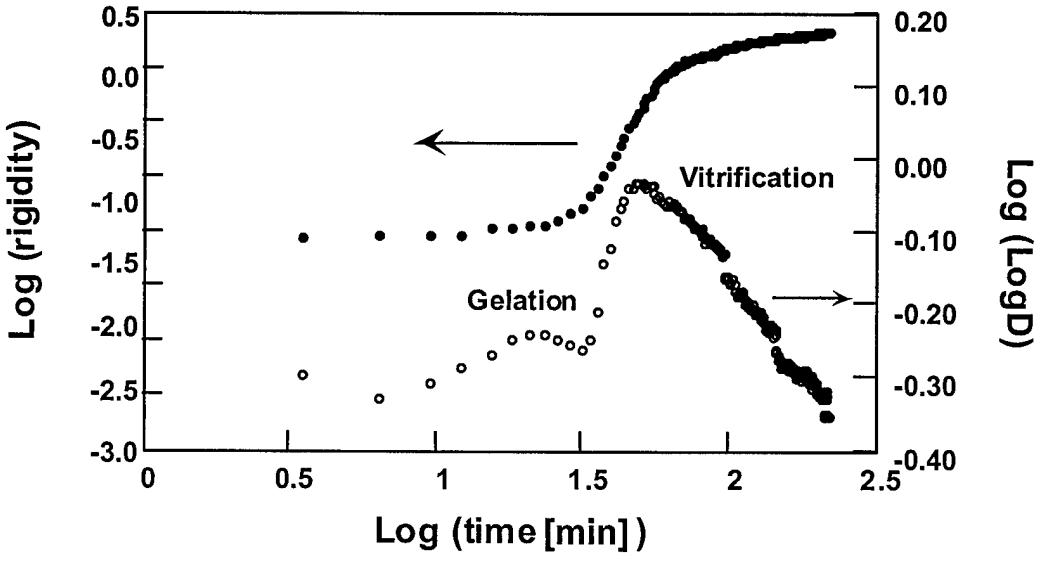

Figure 15. Typical response observed from a TBA experiment for the isothermal cure (40 °C) of a glass braid specimen impregnated with vinyl-ester resin.

5.2.2 Glass Transition Temperature vs. Degree of Cure

The increase in T_g was measured from the initial uncured state of the resin to the final glassy state. The initial T_g, T_g^o, was measured at -25 °C, and the maximum T_g, T_g^∞, was measured at 125 °C. Other studies of various vinyl-ester systems have reported similar T_g values (Hong and Chung 1991; Lee and Lee 1994). Also, T_g^∞ for pure vinyl ester was measured at 137 °C, and T_g^∞ for pure styrene was measured at 100 °C; therefore, 125 °C is a logical value for the mixture.

Figure 16 shows the relationship of T_g with time for cure temperatures of 20°, 30°, and 40 °C. The solid lines were generated from a $T_g(\alpha)$ model fit (discussed later). The T_g increases rapidly at first, and then slightly above vitrification, the increase in T_g becomes much slower. By definition, vitrification corresponds to the point where the T_g reaches the cure temperature ($T_g = T_{cure}$). After the glass has formed, the rate of T_g increase slows considerably. However, at this point, the reaction has not necessarily been terminated. To illustrate the increase in T_g over an extended time, a 40 °C isothermal cure was carried out for 5580 min (73 hr). Figure 16 shows that the T_g at 242 min was measured at 65 °C. After 5580 min, the T_g was measured at 78 °C. Thus, approximately a 15% increase in T_g was realized over this extended cure period. This increase could be very important during long-term, room-temperature part storage or during aging.

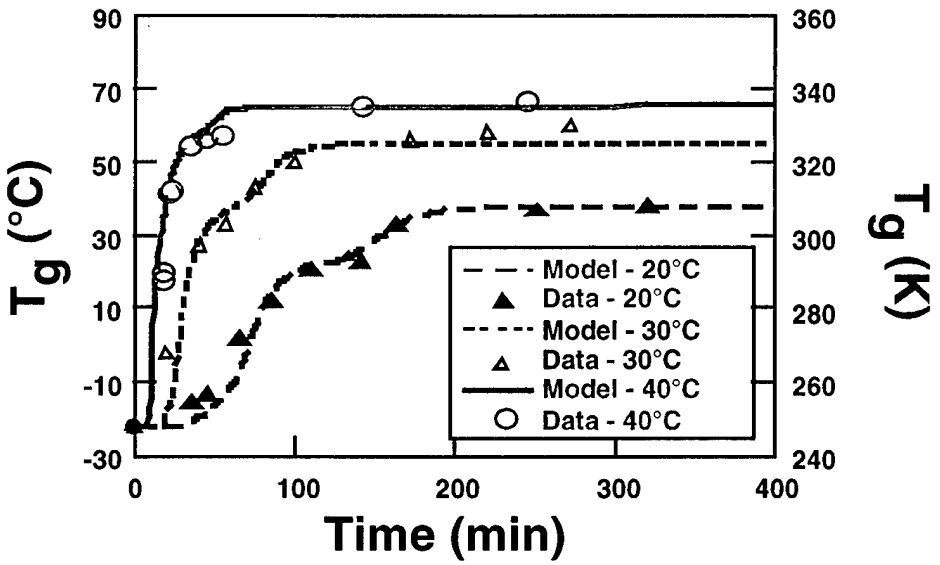

Figure 16. T_g vs. time for vinyl-ester resin. Data points taken with the TBA and the solid lines are based on a $T_g(\alpha)$ model fit.

It was mentioned previously that the vitrification point as measured in the TBA occurs earlier than the leveling off of the degree of cure, as measured in the DSC. This leveling off is often assumed to indicate the vitrification. This may be an

accurate estimation for many epoxy resins, but is not accurate for the vinyl-ester resin system. In Figure 16, the T_g approaches a plateau immediately after vitrification ($T_g = T_{cure}$), but begins to increase again before approaching a final plateau. The first plateau is reached when the vinyl-ester reaction terminates, thus slowing down the T_g increase. However, the styrene reaction continues and further increases the T_g. The first plateau coincides directly with the vitrification point measured in the TBA ($T_g = T_{cure}$), and the second plateau coincides directly with the leveling off, as seen in the degree of cure from the DSC.

It has been suggested that the T_g could be used to monitor the reaction progress much like the degree of cure (Gillham and Enns 1994). The T_g has the advantage of being much more sensitive in the later stages of the cure. However, a direct relationship between the degree of cure and T_g must exist to use this technique. Because of the competing reactions involving the styrene and vinyl ester, the relationship between T_g and degree of cure is only direct for a specific cure temperature. Thus, the relationship between T_g and degree of cure for a typical nonisothermal cure would depend on the temperature history. This greatly limits the use of T_g as a conversion measurement by restricting its application to isothermal conditions. This temperature dependency also means that greater care must be used during production to achieve consistent and predictable part quality.

The vinyl-ester cure process was stopped by quenching the specimen at various stages of cure using liquid nitrogen. The T_g at this cure stage was measured in the TBA by increasing the temperature up through the T_g at 2 °C/min. The T_g was then plotted against the degree of cure for each isothermal temperature (see Figure 17). For other thermosets, such as epoxy and polyimide systems, the data points for various isothermal temperatures have been found to collapse on one master curve (Gillham and Enns 1994; Zukas 1994). However, as shown in Figure 17, this was not the case with the current system due to the competing reaction mechanism explained previously.

The degree of cure axis, shown in Figure 17, can be divided into three regions. The first region shows a rapid increase in the T_g for a very small increase in conversion. Region 1 represents the period before and near gelation, where significant physical changes are occurring in the resin, but chemical conversion is not yet significant. Region 2 shows a small increase in the T_g over a large increase in the conversion. This region corresponds to the maximum rate of change in degree of cure, as shown in Figure 7. Region 2 occurs when the material passes through vitrification and approaches the maximum degree of cure that can be measured using DSC. There is evidence that the T_g and, consequently, degree of cure, continue to increase during extended isothermal cures. If it is assumed that the T_g will increase to T_g^∞ over an extended cure time and that the styrene conversion will slowly increase to unity, the endpoints shown in Figure 17 can be fixed. Region 3 represents the time frame when T_g

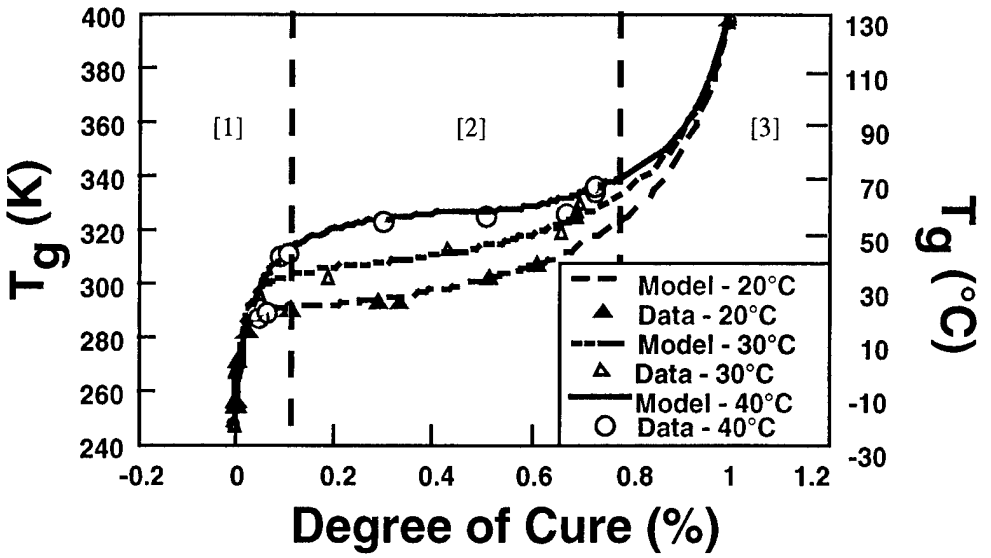

Figure 17. Glass transition temperature vs. degree of cure. It is assumed that the degree of cure continues to increase to 1.0, and the T_g continues to increase to T_g^{∞}. The solid lines represent the $T_g(\alpha)$ model fit.

and degree of cure approach their ultimate values at similar rates. Based on the complicated reaction mechanism of the vinyl ester, there is a possibility that various morphologies are being formed in these three separate regions. Further study into this area is necessary.

Even though it was found that the T_g and degree of cure did not exhibit a direct relationship for this particular system, it was still desirable to develop an emperical model from the data. A mathematical expression describing the T_g explicitly in terms of the degree of cure is particularly convenient for implementation in cure-dependant residual stress modeling. Equation 12 was chosen because it has been successfully used by other investigators (Hong and Chung 1991; Gillham and Enns 1994; Zukas 1994).

$$\ln(T_g) = \frac{(1-\alpha)\ln(T_g^o) + \left(\frac{\Delta c_p^{\infty}}{\Delta c_p^o}\right)\alpha\ln(T_g^{\infty})}{(1-\alpha) + \left(\frac{\Delta c_p^{\infty}}{\Delta c_p^o}\right)\alpha}. \qquad (12)$$

In equation 12, the term $(\Delta c_p^{\infty} / \Delta c_p^o)$ is used as a fitting parameter in this study. The data was fit to equation 12 in two separate regions, before vitrification ($0<\alpha<\alpha_{vit}$) and after vitrification ($\alpha_{vit}<\alpha<1$). The solid lines in Figure 17 represent the fit of this equation to the experimental data. The parameters that were used for the fit are given in Table 5. There are two fitting parameters in each region of

Table 5. Parameters for the $T_g(\alpha)$ model for vinyl ester, given in Kelvin.

Temp. (K)	$(0< \alpha <\alpha_{vit})$			$(\alpha_{vit} <\alpha<1)$		
	$(\Delta c_p^{\infty} / \Delta c_p^{o})_1$	$(T_g^{o})_1$	$(T_g^{\infty})_1$	$(\Delta c_p^{\infty} / \Delta c_p^{o})_2$	$(T_g^{o})_2$	$(T_g^{\infty})_2$
273	150	248.15	274.15	0.15	287.15	378.15
303	100	248.15	308.15	0.15	303.15	378.15
313	35	248.15	330.15	0.15	317.15	378.15

the model, and the parameters (T_g^{o}) and (T_g^{∞}) are defined as the experimentally measured initial and final glass transition temperatures, respectively. The fit of the T_g vs. time curve (Figure 16) was generated from this model and follows the experimental data well.

5.2.3 TTT Diagram—Times to Gelation and Vitrification

The gelation and vitrification times were measured in the TBA for cure temperatures between 20° and 60 °C. The average time to the gelation and vitrification transitions are given in Table 6.

Table 6. Average times to gelation and vitrification for vinyl-ester resin.

Cure Temperature (°C)	Average Gelation (min)	Average Vitrification (min)
20	47.67 + 7.12	137.75 + 17.27
30	26.00 + 4.24	56.50 + 5.51
40	13.00 + 0.00	20.00 + 1.41
50	—	15.00 + 0.00
60	—	11.50 + 2.12

Figure 18 shows a portion of the TTT diagram for the vinyl-ester system. It was not possible to experimentally show the upper section of the diagram. When the isothermal cure temperature was increased above 60 °C, a different curing mechanism was observed than that at lower temperatures. This high-temperature curing reaction was not studied in this investigation, nor was the reaction below 20 °C. The experimental values for T_g^{o} and T_g^{∞} are shown as the limits of the TTT diagram at -25° and 125 °C, respectively.

The gelation for isothermal curing temperatures above 40 °C could not be measured because of the fast nature of the reaction; however, if the gelation data points are extended, the ${}_{gel}T_g$ can be estimated at approximately -5 °C. When

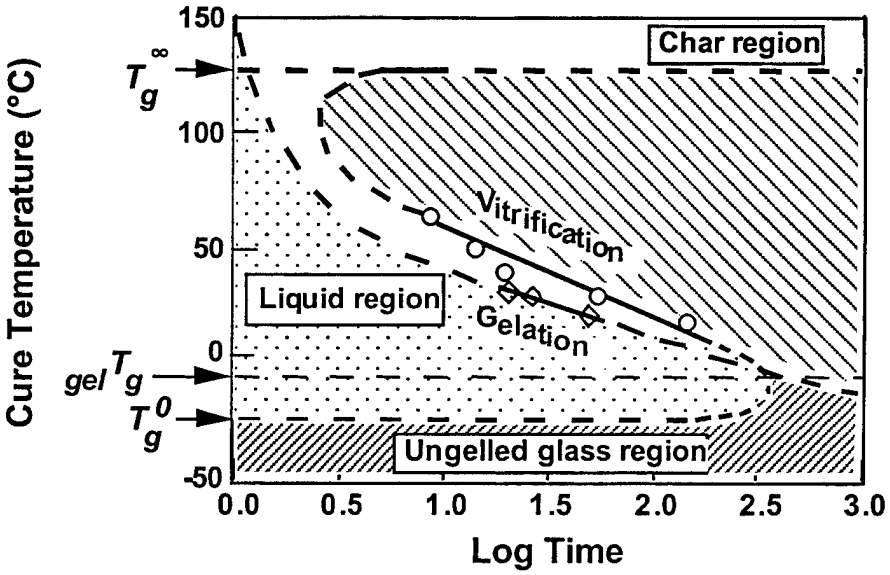

Figure 18. General shape of the TTT diagram. Only data in the intermediate region were collected.

plotted on a log-time TTT diagram (Figure 18), the gelation time exhibits a linear decrease with increasing cure temperature, given by the following equation:

$$log(t_{gel}) = 2.249 - 0.0282T_{cure}. \quad (13)$$

In the same region, the vitrification points also show a linear behavior, given by

$$log(t_{vit}) = 2.585 - 0.0274T_{cure}. \quad (14)$$

The TTT diagram is useful in defining a material's processing window. More specifically, equation 13 can be used to estimate times (for a given cure temperature) that would be required to infuse a part before gelation took place.

6. Conclusions

A number of conclusions were made from the investigation of the vinyl-ester resin system. First, it was shown that the overall cure reaction is consistent with an autocatalytic behavior. The cure rate increased to a maximum value and then decreased. A traditional autocatalytic model fit the data when a modification was made to account for a maximum extent of cure, α_{max}, which is less than one. The inhibitor in the resin system was found to be more effective at lower curing temperatures. The time to deplete the inhibitor in the system as a function of

cure temperature was modeled using an Arrhenius temperature distribution. The combination of the kinetic autocatalytic model and the inhibitor depletion model resulted in an accurate description of the cure reaction.

The curing reaction was found to continue long after the DSC was capable of accurately measuring the heat of reaction. TBA proved to be very sensitive and was able to detect physical changes occurring in these later curing stages. The T_g did not reach its maximum value at any of the temperatures studied for the time durations measured. However, there is evidence that the T_g is still increasing over extended cure times and could reach its ultimate value.

The vinyl-ester curing mechanism was found to have competing reactions occurring between the vinyl ester and styrene. The formation of microgels at early stages in the cure may have affected the progress of the cure. This could contribute to the unusual changes in the reaction rate that were seen in the DSC thermograms. The vinyl-ester curing mechanism was also found to be temperature dependent, thus complicating the extension of isothermal cure models to nonisothermal cases. The T_g was found to increase in a path, depending on the isothermal cure temperature. This limited the use of T_g as an alternative measure of conversion.

The T_g for each isothermal temperature was modeled as a function of the degree of cure using a commonly used expression. Because of the shape of the $T_g(\alpha)$ curve for the vinyl-ester resin, this equation was applied in two regions, before vitrification and after vitrification. In addition to understanding the relationship between the T_g and degree of cure, this model is particularly convenient for implementation in cure-dependant residual-stress modeling.

Room-temperature curing resins have not been studied as extensively as higher temperature systems. The cure reaction has proven to be significantly different than higher temperature reactions and very sensitive to temperature. Continued investigations into the curing mechanism and the resulting mechanical properties would help to fully understand the low-temperature reactions and the effects of processing conditions. Also, studies that investigate the morphologies that develop at various cure stages may give further insight into the formation of the vinyl-ester structure.

INTENTIONALLY LEFT BLANK.

7. References

Brill, R. P., R. L. McCullough, and G. R. Palmese. "Effect of Resin Formulation and Reaction Temperature on the Curing Kinetics of Vinyl-Ester Resins." *Proceedings, American Society of Composites, 11th Annual Technical Conference,* p. 576, October 1996.

Dillman, S. H., and J. C. Seferis. "Kinetic Viscoelasticity for the Dynamic Mechanical Properties of Polymer Systems." *Journal of Macromolecular Science-Chemistry,* September 1987.

Gillham, J. K., and J. B. Enns. "On the Cure and Properties of Thermosetting Polymers Using Torsional Braid Analysis." *Trends in Polymer Science,* vol. 2, no. 12, December 1994.

Han, C. D., and K. W. Lem. "Curing Kinetics of Unsaturated Polyester and Vinyl-Ester Resins." *Chemorheology of Thermosetting Polymers,* edited by C. A. May, American Chemical Society, Washington, DC, pp. 201–221, 1983.

Hong, M. S., and I. J. Chung. "The Cure Behavior of Vinyl-Ester Resin With Low Profile Additive I. Cure Kinetics and TTT Cure Diagram." *Polymer Journal,* vol. 23, no. 6, pp. 747–755, 1991.

Kamal, M. R., and S. Sourour. "Kinetics and Thermal Characterization of Thermoset Cure." *Polymer Engineering and Science,* vol. 13, no. 1, pp. 57–64, 1973.

Lee, D., and C. D. Han. "A Chemorheological Model for the Cure of Unsaturated Polyester Resin." *Polymer Engineering and Science,* vol. 27, no. 13, July 1987.

Lee, J. H., and J. W. Lee. "Kinetic Parameters Estimation for Cure Reaction of Epoxy Based Vinyl-Ester Resin." *Polymer Engineering and Science,* vol. 34, no. 7, pp. 742–749, May 1994.

Levenspiel, O. *Chemical Reaction Engineering, 2nd ed.* New York: John Wiley and Sons, 1972.

Michaud, D. J. "Investigation of Curing Behavior in Thick Thermoset Composites Manufactured by Resin Transfer Molding." Master's thesis, University of Delaware, Newark, DE, 1996.

Palmese, G. R., O. A. Andersen, and V. M. Karbhari. "Effect of Glass Fiber Sizing on the Cure Kinetics of Vinyl-Ester Resins." *Composites Part A: Applied Science and Manufacturing,* vol. 30, no. 1, pp. 11–18, 1998.

Stevens, M. P. *Polymer Chemistry, An Introduction, 2nd ed.* New York: Oxford University Press, pp. 70–103, 1990.

Stone, M. A. "Thermo-Chemical and Thermo-Mechanical Response of Reacting Polymers." Master's thesis, University of Delaware, Newark, DE, 1997.

Yi, S., H. H. Hilton, and M. F. Ahmad. "Curing Process Induced Viscoelastic Residual Stress in Polymer Matrix Laminated Composites." Submitted to *ASME Journal of Applied Mechanics,* 1995.

Ziaee, S., and G. R. Palmese. "Effects of Temperature on Cure Kinetics and Mechanical Properties of Vinyl-Ester Resins." *Journal of Polymer Science, Part B: Polymer Physics,* vol. 37, no. 7, pp. 725–744, 1999.

Zukas, W. "Torsional Braid Analysis of the Aromatic Amine Cure of Epoxy Resins." *Journal of Applied Polymer Science,* vol. 53, pp. 429–440, 1994.

NO. OF COPIES	ORGANIZATION
2	DEFENSE TECHNICAL INFORMATION CENTER DTIC OCA 8725 JOHN J KINGMAN RD STE 0944 FT BELVOIR VA 22060-6218
1	HQDA DAMO FDT 400 ARMY PENTAGON WASHINGTON DC 20310-0460
1	OSD OUSD(A&T)/ODDR&E(R) DR R J TREW 3800 DEFENSE PENTAGON WASHINGTON DC 20301-3800
1	COMMANDING GENERAL US ARMY MATERIEL CMD AMCRDA TF 5001 EISENHOWER AVE ALEXANDRIA VA 22333-0001
1	INST FOR ADVNCD TCHNLGY THE UNIV OF TEXAS AT AUSTIN 3925 W BRAKER LN STE 400 AUSTIN TX 78759-5316
1	US MILITARY ACADEMY MATH SCI CTR EXCELLENCE MADN MATH THAYER HALL WEST POINT NY 10996-1786
1	DIRECTOR US ARMY RESEARCH LAB AMSRL D DR D SMITH 2800 POWDER MILL RD ADELPHI MD 20783-1197
1	DIRECTOR US ARMY RESEARCH LAB AMSRL CI AI R 2800 POWDER MILL RD ADELPHI MD 20783-1197

NO. OF COPIES	ORGANIZATION
3	DIRECTOR US ARMY RESEARCH LAB AMSRL CI LL 2800 POWDER MILL RD ADELPHI MD 20783-1197
3	DIRECTOR US ARMY RESEARCH LAB AMSRL CI IS T 2800 POWDER MILL RD ADELPHI MD 20783-1197
	ABERDEEN PROVING GROUND
2	DIR USARL AMSRL CI LP (BLDG 305)

NO. OF COPIES	ORGANIZATION
1	DIRECTOR US ARMY RESEARCH LAB AMSRL CP CA D SNIDER 2800 POWDER MILL RD ADELPHI MD 20783-1145
1	DIRECTOR US ARMY RESEARCH LAB AMSRL CI IS R 2800 POWDER MILL RD ADELPHI MD 20783-1145
3	DIRECTOR US ARMY RESEARCH LAB AMSRL OP SD TL 2800 POWDER MILL RD ADELPHI MD 20783-1145
1	DPTY ASST SECY FOR R&T SARD TT THE PENTAGON RM 3EA79 WASHINGTON DC 20301-7100
1	COMMANDER US ARMY MATERIEL CMD AMXMI INT 5001 EISENHOWER AVE ALEXANDRIA VA 22333-0001
4	COMMANDER US ARMY ARDEC AMSTA AR CC G PAYNE J GEHBAUER C BAULIEU H OPAT PICATINNY ARSENAL NJ 07806-5000
2	COMMANDER US ARMY ARDEC AMSTA AR AE WW E BAKER J PEARSON PICATINNY ARSENAL NJ 07806-5000

NO. OF COPIES	ORGANIZATION
1	COMMANDER US ARMY ARDEC AMSTA AR FSE PICATINNY ARSENAL NJ 07806-5000
1	COMMANDER US ARMY ARDEC AMSTA AR TD C SPINELLI PICATINNY ARSENAL NJ 07806-5000
6	COMMANDER US ARMY ARDEC AMSTA AR CCH A W ANDREWS S MUSALLI R CARR M LUCIANO E LOGSDEN T LOUZEIRO PICATINNY ARSENAL NJ 07806-5000
1	COMMANDER US ARMY ARDEC AMSTA AR CCH P J LUTZ PICATINNY ARSENAL NJ 07806-5000
1	COMMANDER US ARMY ARDEC AMSTA AR FSF T C LIVECCHIA PICATINNY ARSENAL NJ 07806-5000
1	COMMANDER US ARMY ARDEC AMSTA ASF PICATINNY ARSENAL NJ 07806-5000
1	COMMANDER US ARMY ARDEC AMSTA AR QAC T C C PATEL PICATINNY ARSENAL NJ 07806-5000

NO. OF COPIES	ORGANIZATION
1	COMMANDER US ARMY ARDEC AMSTA AR M D DEMELLA PICATINNY ARSENAL NJ 07806-5000
3	COMMANDER US ARMY ARDEC AMSTA AR FSA A WARNASH B MACHAK M CHIEFA PICATINNY ARSENAL NJ 07806-5000
2	COMMANDER US ARMY ARDEC AMSTA AR FSP G M SCHIKSNIS D CARLUCCI PICATINNY ARSENAL NJ 07806-5000
1	COMMANDER US ARMY ARDEC AMSTA AR FSP A P KISATSKY PICATINNY ARSENAL NJ 07806-5000
2	COMMANDER US ARMY ARDEC AMSTA AR CCH C H CHANIN S CHICO PICATINNY ARSENAL NJ 07806-5000
1	COMMANDER US ARMY ARDEC AMSTA AR QAC T D RIGOGLIOSO PICATINNY ARSENAL NJ 07806-5000
1	COMMANDER US ARMY ARDEC AMSTA AR WET T SACHAR BLDG 172 PICATINNY ARSENAL NJ 07806-5000

NO. OF COPIES	ORGANIZATION
1	US ARMY ARDEC INTELLIGENCE SPECIALIST AMSTA AR WEL F M GUERRIERE PICATINNY ARSENAL NJ 07806-5000
9	COMMANDER US ARMY ARDEC AMSTA AR CCH B P DONADIA F DONLON P VALENTI C KNUTSON G EUSTICE S PATEL G WAGNECZ R SAYER F CHANG PICATINNY ARSENAL NJ 07806-5000
6	COMMANDER US ARMY ARDEC AMSTA AR CCL F PUZYCKI R MCHUGH D CONWAY E JAROSZEWSKI R SCHLENNER M CLUNE PICATINNY ARSENAL NJ 07806-5000
5	PM SADARM SFAE GCSS SD COL B ELLIS M DEVINE W DEMASSI J PRITCHARD S HROWNAK PICATINNY ARSENAL NJ 07806-5000
2	PEO FIELD ARTILLERY SYS SFAE FAS PM H GOLDMAN T MCWILLIAMS PICATINNY ARSENAL NJ 07806-5000

NO. OF COPIES	ORGANIZATION
1	COMMANDER US ARMY ARDEC AMSTA AR WEA J BRESCIA PICATINNY ARSENAL NJ 07806-5000
12	PM TMAS SFAE GSSC TMA R MORRIS C KIMKER D GUZIEWICZ E KOPACZ R ROESER R DARCY R KOWALSKI R MCDANOLDS L D ULISSE C ROLLER J MCGREEN B PATTER PICATINNY ARSENAL NJ 07806-5000
1	COMMANDER US ARMY ARDEC PRODUCTION BASE MODERN ACTY AMSMC PBM K PICATINNY ARSENAL NJ 07806-5000
1	COMMANDER US ARMY TACOM PM ABRAMS SFAE ASM AB 6501 ELEVEN MILE RD WARREN MI 48397-5000
1	COMMANDER US ARMY TACOM AMSTA SF WARREN MI 48397-5000
1	COMMANDER US ARMY TACOM PM BFVS SFAE GCSS W BV 6501 ELEVEN MILE RD WARREN MI 48397-5000

NO. OF COPIES	ORGANIZATION
1	DIRECTOR AIR FORCE RESEARCH LAB MLLMD D MIRACLE 2230 TENTH ST WRIGHT PATTERSON AFB OH 45433-7817
1	OFC OF NAVAL RESEARCH J CHRISTODOULOU ONR CODE 332 800 N QUINCY ST ARLINGTON VA 22217-5600
1	US ARMY CERL R LAMPO 2902 NEWMARK DR CHAMPAIGN IL 61822
1	COMMANDER US ARMY TACOM PM SURVIVABLE SYSTEMS SFAE GCSS W GSI H M RYZYI 6501 ELEVEN MILE RD WARREN MI 48397-5000
1	COMMANDER US ARMY TACOM CHIEF ABRAMS TESTING SFAE GCSS W AB QT T KRASKIEWICZ 6501 ELEVEN MILE RD WARREN MI 48397-5000
1	COMMANDER WATERVLIET ARSENAL SMCWV QAE Q B VANINA BLDG 44 WATERVLIET NY 12189-4050
3	ARMOR SCHOOL ATZK TD R BAUEN J BERG A POMEY FT KNOX KY 40121

NO. OF COPIES	ORGANIZATION
2	HQ IOC TANK AMMUNITION TEAM AMSIO SMT R CRAWFORD W HARRIS ROCK ISLAND IL 61299-6000
2	COMMANDER US ARMY AMCOM AVIATION APPLIED TECH DIR J SCHUCK FT EUSTIS VA 23604-5577
14	COMMANDER US ARMY TACOM AMSTA TR R R MCCLELLAND D THOMAS J BENNETT D HANSEN AMSTA JSK S GOODMAN J FLORENCE K IYER D TEMPLETON A SCHUMACHER AMSTA TR D D OSTBERG L HINOJOSA B RAJU AMSTA CS SF H HUTCHINSON F SCHWARZ WARREN MI 48397-5000
14	BENET LABORATORIES AMSTA AR CCB R FISCELLA M SOJA E KATHE M SCAVULO G SPENCER P WHEELER S KRUPSKI J VASILAKIS G FRIAR R HASENBEIN AMSTA CCB R S SOPOK E HYLAND D CRAYON R DILLON WATERVLIET NY 12189-4050

NO. OF COPIES	ORGANIZATION
1	DIRECTOR US ARMY AMCOM SFAE AV RAM TV D CALDWELL BLDG 5300 REDSTONE ARSENAL AL 35898
1	NAVAL SURFACE WARFARE CTR DAHLGREN DIV CODE G06 DAHLGREN VA 22448
2	US ARMY CORPS OF ENGINEERS CERD C T LIU CEW ET T TAN 20 MASS AVE NW WASHINGTON DC 20314
1	US ARMY COLD REGIONS RSCH & ENGRNG LAB P DUTTA 72 LYME RD HANOVER NH 03755
1	USA SBCCOM PM SOLDIER SPT AMSSB PM RSS A J CONNORS KANSAS ST NATICK MA 01760-5057
2	USA SBCCOM MATERIAL SCIENCE TEAM AMSSB RSS J HERBERT M SENNETT KANSAS ST NATICK MA 01760-5057
2	OFC OF NAVAL RESEARCH D SIEGEL CODE 351 J KELLY 800 N QUINCY ST ARLINGTON VA 22217-5660
1	NAVAL SURFACE WARFARE CTR TECH LIBRARY CODE 323 17320 DAHLGREN RD DAHLGREN VA 22448

NO. OF COPIES	ORGANIZATION
1	NAVAL SURFACE WARFARE CTR CRANE DIVISION M JOHNSON CODE 20H4 LOUISVILLE KY 40214-5245
2	NAVAL SURFACE WARFARE CTR U SORATHIA C WILLIAMS CD 6551 9500 MACARTHUR BLVD WEST BETHESDA MD 20817
2	COMMANDER NAVAL SURFACE WARFARE CTR CARDEROCK DIVISION R PETERSON CODE 2020 M CRITCHFIELD CODE 1730 BETHESDA MD 20084
8	DIRECTOR US ARMY NATIONAL GROUND INTELLIGENCE CTR D LEITER MS 404 M HOLTUS MS 301 M WOLFE MS 307 S MINGLEDORF MS 504 J GASTON MS 301 W GSTATTENBAUER MS 304 R WARNER MS 305 J CRIDER MS 306 220 SEVENTH ST NE CHARLOTTESVILLE VA 22091
1	NAVAL SEA SYSTEMS CMD D LIESE 2531 JEFFERSON DAVIS HWY ARLINGTON VA 22242-5160
1	NAVAL SURFACE WARFARE CTR M LACY CODE B02 17320 DAHLGREN RD DAHLGREN VA 22448
1	EXPEDITIONARY WARFARE DIV N85 F SHOUP 2000 NAVY PENTAGON WASHINGTON DC 20350-2000

NO. OF COPIES	ORGANIZATION
8	US ARMY SBCCOM SOLDIER SYSTEMS CENTER BALLISTICS TEAM J WARD W ZUKAS P CUNNIFF J SONG MARINE CORPS TEAM J MACKIEWICZ BUS AREA ADVOCACY TEAM W HASKELL AMSSB RCP SS W NYKVIST S BEAUDOIN KANSAS ST NATICK MA 01760-5019
9	US ARMY RESEARCH OFC A CROWSON H EVERETT J PRATER G ANDERSON D STEPP D KISEROW J CHANG PO BOX 12211 RESEARCH TRIANGLE PARK NC 27709-2211
8	NAVAL SURFACE WARFARE CTR J FRANCIS CODE G30 D WILSON CODE G32 R D COOPER CODE G32 J FRAYSSE CODE G33 E ROWE CODE G33 T DURAN CODE G33 L DE SIMONE CODE G33 R HUBBARD CODE G33 DAHLGREN VA 22448
2	NAVAL SURFACE WARFARE CTR CARDEROCK DIVISION R CRANE CODE 2802 C WILLIAMS CODE 6553 3A LEGGETT CIR BETHESDA MD 20054-5000
1	AFRL MLBC 2941 P ST RM 136 WRIGHT PATTERSON AFB OH 45433-7750

NO. OF COPIES	ORGANIZATION
1	AFRL MLSS R THOMSON 2179 12TH ST RM 122 WRIGHT PATTERSON AFB OH 45433-7718
2	AFRL F ABRAMS J BROWN BLDG 653 2977 P ST STE 6 WRIGHT PATTERSON AFB OH 45433-7739
1	WATERWAYS EXPERIMENT D SCOTT 3909 HALLS FERRY RD SC C VICKSBURG MS 39180
5	DIRECTOR LLNL R CHRISTENSEN S DETERESA F MAGNESS M FINGER MS 313 M MURPHY L 282 PO BOX 808 LIVERMORE CA 94550
1	AFRL MLS OL L COULTER 7278 4TH ST BLDG 100 BAY D HILL AFB UT 84056-5205
1	OSD JOINT CCD TEST FORCE OSD JCCD R WILLIAMS 3909 HALLS FERRY RD VICKSBURG MS 29180-6199
3	DARPA M VANFOSSEN S WAX L CHRISTODOULOU 3701 N FAIRFAX DR ARLINGTON VA 22203-1714
1	DIRECTOR LOS ALAMOS NATIONAL LAB F L ADDESSIO T 3 MS 5000 PO BOX 1633 LOS ALAMOS NM 87545

NO. OF COPIES	ORGANIZATION
2	SERDP PROGRAM OFC PM P2 C PELLERIN B SMITH 901 N STUART ST STE 303 ARLINGTON VA 22203
1	US DEPT OF ENERGY OFC OF ENVIRONMENTAL MANAGEMENT P RITZCOVAN 19901 GERMANTOWN RD GERMANTOWN MD 20874-1928
1	OAK RIDGE NATIONAL LABORATORY R M DAVIS PO BOX 2008 OAK RIDGE TN 37831-6195
1	OAK RIDGE NATIONAL LABORATORY C EBERLE MS 8048 PO BOX 2008 OAK RIDGE TN 37831
3	DIRECTOR SANDIA NATIONAL LABS APPLIED MECHANICS DEPT MS 9042 J HANDROCK Y R KAN J LAUFFER PO BOX 969 LIVERMORE CA 94551-0969
1	OAK RIDGE NATIONAL LABORATORY C D WARREN MS 8039 PO BOX 2008 OAK RIDGE TN 37831
4	NIST M VANLANDINGHAM MS 8621 J CHIN MS 8621 J MARTIN MS 8621 D DUTHINH MS 8611 100 BUREAU DR GAITHERSBURG MD 20899

NO. OF COPIES	ORGANIZATION
1	HYDROGEOLOGIC INC SERDP ESTCP SPT OFC S WALSH 1155 HERNDON PKWY STE 900 HERNDON VA 20170
3	NASA LANGLEY RSCH CTR AMSRL VS W ELBER MS 266 F BARTLETT JR MS 266 G FARLEY MS 266 HAMPTON VA 23681-0001
1	NASA LANGLEY RSCH CTR T GATES MS 188E HAMPTON VA 23661-3400
1	FHWA E MUNLEY 6300 GEORGETOWN PIKE MCLEAN VA 22101
1	USDOT FEDERAL RAILRD M FATEH RDV 31 WASHINGTON DC 20590
3	CYTEC FIBERITE R DUNNE D KOHLI R MAYHEW 1300 REVOLUTION ST HAVRE DE GRACE MD 21078
1	MARINE CORPS INTLLGNC ACTVTY D KOSITZKE 3300 RUSSELL RD STE 250 QUANTICO VA 22134-5011
1	DIRECTOR NATIONAL GRND INTLLGNC CTR IANG TMT 220 SEVENTH ST NE CHARLOTTESVILLE VA 22902-5396
1	SIOUX MFG B KRIEL PO BOX 400 FT TOTTEN ND 58335

NO. OF COPIES	ORGANIZATION
2	3TEX CORPORATION A BOGDANOVICH J SINGLETARY 109 MACKENAN DR CARY NC 27511
1	3M CORPORATION J SKILDUM 3M CENTER BLDG 60 IN 01 ST PAUL MN 55144-1000
1	DIRECTOR DEFENSE INTLLGNC AGNCY TA 5 K CRELLING WASHINGTON DC 20310
1	ADVANCED GLASS FIBER YARNS T COLLINS 281 SPRING RUN LANE STE A DOWNINGTON PA 19335
1	COMPOSITE MATERIALS INC D SHORTT 19105 63 AVE NE PO BOX 25 ARLINGTON WA 98223
1	JPS GLASS L CARTER PO BOX 260 SLATER RD SLATER SC 29683
1	COMPOSITE MATERIALS INC R HOLLAND 11 JEWEL CT ORINDA CA 94563
1	COMPOSITE MATERIALS INC C RILEY 14530 S ANSON AVE SANTA FE SPRINGS CA 90670
2	SIMULA J COLTMAN R HUYETT 10016 S 51ST ST PHOENIX AZ 85044

NO. OF COPIES	ORGANIZATION
2	PROTECTION MATERIALS INC M MILLER F CRILLEY 14000 NW 58 CT MIAMI LAKES FL 33014
2	FOSTER MILLER M ROYLANCE W ZUKAS 195 BEAR HILL RD WALTHAM MA 02354-1196
1	ROM DEVELOPMENT CORP R O MEARA 136 SWINEBURNE ROW BRICK MARKET PLACE NEWPORT RI 02840
2	TEXTRON SYSTEMS T FOLTZ M TREASURE 1449 MIDDLESEX ST LOWELL MA 01851
1	O GARA HESS & EISENHARDT M GILLESPIE 9113 LESAINT DR FAIRFIELD OH 45014
2	MILLIKEN RSCH CORP H KUHN M MACLEOD PO BOX 1926 SPARTANBURG SC 29303
1	CONNEAUGHT INDUSTRIES INC J SANTOS PO BOX 1425 COVENTRY RI 02816
1	BATTELLE NATICK OPNS B HALPIN 209 W CENTRAL ST STE 302 NATICK MA 01760
1	ARMTEC DEFENSE PRODUCTS S DYER 85 901 AVE 53 PO BOX 848 COACHELLA CA 92236

NO. OF COPIES	ORGANIZATION
1	NATIONAL COMPOSITE CENTER T CORDELL 2000 COMPOSITE DR KETTERING OH 45420
3	PACIFIC NORTHWEST LAB M SMITH G VAN ARSDALE R SHIPPELL PO BOX 999 RICHLAND WA 99352
2	AMOCO PERFORMANCE PRODUCTS M MICHNO JR J BANISAUKAS 4500 MCGINNIS FERRY RD ALPHARETTA GA 30202-3944
8	ALLIANT TECHSYSTEMS INC C CANDLAND MN11 2830 C AAKHUS MN11 2830 B SEE MN11 2439 N VLAHAKUS MN11 2145 R DOHRN MN11 2830 S HAGLUND MN11 2439 M HISSONG MN11 2830 D KAMDAR MN11 2830 600 SECOND ST NE HOPKINS MN 55343-8367
1	SAIC M PALMER 1410 SPRING HILL RD STE 400 MS SH4 5 MCLEAN VA 22102
1	SAIC G CHRYSSOMALLIS 3800 W 80TH ST STE 1090 BLOOMINGTON MN 55431
1	AAI CORPORATION T G STASTNY PO BOX 126 HUNT VALLEY MD 21030-0126
1	APPLIED COMPOSITES W GRISCH 333 NORTH SIXTH ST ST CHARLES IL 60174

NO. OF COPIES	ORGANIZATION
1	CUSTOM ANALYTICAL ENG SYS INC A ALEXANDER 13000 TENSOR LANE NE FLINTSTONE MD 21530
1	OFC DEPUTY UNDER SEC DEFNS J THOMPSON 1745 JEFFERSON DAVIS HWY CRYSTAL SQ 4 STE 501 ARLINGTON VA 22202
3	ALLIANT TECHSYSTEMS INC J CONDON E LYNAM J GERHARD WV01 16 STATE RT 956 PO BOX 210 ROCKET CENTER WV 26726-0210
1	PROJECTILE TECHNOLOGY INC 515 GILES ST HAVRE DE GRACE MD 21078
3	HEXCEL INC R BOE PO BOX 18748 SALT LAKE CITY UT 84118
5	AEROJET GEN CORP D PILLASCH T COULTER C FLYNN D RUBAREZUL M GREINER 1100 WEST HOLLYVALE ST AZUSA CA 91702-0296
1	HERCULES INC HERCULES PLAZA WILMINGTON DE 19894
1	BRIGS COMPANY J BACKOFEN 2668 PETERBOROUGH ST HERNDON VA 22071-2443
1	ZERNOW TECHNICAL SERVICES L ZERNOW 425 W BONITA AVE STE 208 SAN DIMAS CA 91773

NO. OF COPIES	ORGANIZATION
1	GENERAL DYNAMICS OTS L WHITMORE 10101 NINTH ST NORTH ST PETERSBURG FL 33702
3	GENERAL DYNAMICS OTS FLINCHBAUGH DIV E STEINER B STEWART T LYNCH PO BOX 127 RED LION PA 17356
1	GKN AEROSPACE D OLDS 15 STERLING DR WALLINGFORD CT 06492
5	SIKORSKY AIRCRAFT G JACARUSO T CARSTENSAN B KAY S GARBO MS S330A J ADELMANN 6900 MAIN ST PO BOX 9729 STRATFORD CT 06497-9729
1	PRATT & WHITNEY C WATSON 400 MAIN ST MS 114 37 EAST HARTFORD CT 06108
1	AEROSPACE CORP G HAWKINS M4 945 2350 E EL SEGUNDO BLVD EL SEGUNDO CA 90245
2	CYTEC FIBERITE M LIN W WEB 1440 N KRAEMER BLVD ANAHEIM CA 92806
1	UDLP G THOMAS PO BOX 58123 SANTA CLARA CA 95052

NO. OF COPIES	ORGANIZATION
2	UDLP R BARRETT MAIL DROP M53 V HORVATICH MAIL DROP M53 328 W BROKAW RD SANTA CLARA CA 95052-0359
3	UDLP GROUND SYSTEMS DIVISION M PEDRAZZI MAIL DROP N09 A LEE MAIL DROP N11 M MACLEAN MAIL DROP N06 1205 COLEMAN AVE SANTA CLARA CA 95052
4	UDLP R BRYNSVOLD P JANKE MS 170 4800 EAST RIVER RD MINNEAPOLIS MN 55421-1498
2	BOEING ROTORCRAFT P MINGURT P HANDEL 800 B PUTNAM BLVD WALLINGFORD PA 19086
1	BOEING DOUGLAS PRODUCTS DIV L J HART SMITH 3855 LAKEWOOD BLVD D800 0019 LONG BEACH CA 90846-0001
1	LOCKHEED MARTIN SKUNK WORKS D FORTNEY 1011 LOCKHEED WAY PALMDALE CA 93599-2502
1	LOCKHEED MARTIN R FIELDS 1195 IRWIN CT WINTER SPRINGS FL 32708
1	MATERIALS SCIENCES CORP G FLANAGAN 500 OFC CENTER DR STE 250 FT WASHINGTON PA 19034

NO. OF COPIES	ORGANIZATION
1	NORTHRUP GRUMMAN CORP ELECTRONIC SENSORS & SYSTEMS DIV E SCHOCH MS V 16 1745A W NURSERY RD LINTHICUM MD 21090
1	GDLS DIVISION D BARTLE PO BOX 1901 WARREN MI 48090
2	GDLS D REES M PASIK PO BOX 2074 WARREN MI 48090-2074
1	GDLS MUSKEGON OPERATIONS W SOMMERS JR 76 GETTY ST MUSKEGON MI 49442
1	GENERAL DYNAMICS AMPHIBIOUS SYS SURVIVABILITY LEAD G WALKER 991 ANNAPOLIS WAY WOODBRIDGE VA 22191
6	INST FOR ADVANCED TECH H FAIR I MCNAB P SULLIVAN S BLESS W REINECKE C PERSAD 3925 W BRAKER LN STE 400 AUSTIN TX 78759-5316
2	CIVIL ENGR RSCH FOUNDATION PRESIDENT H BERNSTEIN R BELLE 1015 15TH ST NW STE 600 WASHINGTON DC 20005

NO. OF COPIES	ORGANIZATION
1	ARROW TECH ASSO 1233 SHELBURNE RD STE D8 SOUTH BURLINGTON VT 05403-7700
1	R EICHELBERGER CONSULTANT 409 W CATHERINE ST BEL AIR MD 21014-3613
1	UCLA MANE DEPT ENGR IV H T HAHN LOS ANGELES CA 90024-1597
2	UNIV OF DAYTON RESEARCH INST R Y KIM A K ROY 300 COLLEGE PARK AVE DAYTON OH 45469-0168
1	UMASS LOWELL PLASTICS DEPT N SCHOTT 1 UNIVERSITY AVE LOWELL MA 01854
1	IIT RESEARCH CENTER D ROSE 201 MILL ST ROME NY 13440-6916
1	GA TECH RSCH INST GA INST OF TCHNLGY P FRIEDERICH ATLANTA GA 30392
1	MICHIGAN ST UNIV MSM DEPT R AVERILL 3515 EB EAST LANSING MI 48824-1226
1	UNIV OF WYOMING D ADAMS PO BOX 3295 LARAMIE WY 82071

NO. OF COPIES	ORGANIZATION
2	PENN STATE UNIV R MCNITT C BAKIS 212 EARTH ENGR SCIENCES BLDG UNIVERSITY PARK PA 16802
1	PENN STATE UNIV R S ENGEL 245 HAMMOND BLDG UNIVERSITY PARK PA 16801
1	PURDUE UNIV SCHOOL OF AERO & ASTRO C T SUN W LAFAYETTE IN 47907-1282
1	STANFORD UNIV DEPT OF AERONAUTICS & AEROBALLISTICS S TSAI DURANT BLDG STANFORD CA 94305
1	UNIV OF MAINE ADV STR & COMP LAB R LOPEZ ANIDO 5793 AEWC BLDG ORONO ME 04469-5793
1	JOHNS HOPKINS UNIV APPLIED PHYSICS LAB P WIENHOLD 11100 JOHNS HOPKINS RD LAUREL MD 20723-6099
1	UNIV OF DAYTON J M WHITNEY COLLEGE PARK AVE DAYTON OH 45469-0240
5	UNIV OF DELAWARE CTR FOR COMPOSITE MTRLS J GILLESPIE M SANTARE S YARLAGADDA S ADVANI D HEIDER 201 SPENCER LABORATORY NEWARK DE 19716

NO. OF COPIES	ORGANIZATION
1	DEPT OF MATERIALS SCIENCE & ENGINEERING UNIVERSITY OF ILLINOIS AT URBANA CHAMPAIGN J ECONOMY 1304 WEST GREEN ST 115B URBANA IL 61801
1	NORTH CAROLINA STATE UNIV CIVIL ENGINEERING DEPT W RASDORF PO BOX 7908 RALEIGH NC 27696-7908
1	UNIV OF MARYLAND DEPT OF AEROSPACE ENGNRNG A J VIZZINI COLLEGE PARK MD 20742
1	DREXEL UNIV A S D WANG 32ND & CHESTNUT ST PHILADELPHIA PA 19104
3	UNIV OF TEXAS AT AUSTIN CTR FOR ELECTROMECHANICS J PRICE A WALLS J KITZMILLER 10100 BURNET RD AUSTIN TX 78758-4497
3	VA POLYTECHNICAL INST & STATE UNIV DEPT OF ESM M W HYER K REIFSNIDER R JONES BLACKSBURG VA 24061-0219
1	SOUTHWEST RSCH INST ENGR & MATL SCIENCES DIV J RIEGEL 6220 CULEBRA RD PO DRAWER 28510 SAN ANTONIO TX 78228-0510

NO. OF COPIES	ORGANIZATION
	ABERDEEN PROVING GROUND
1	US ARMY MATERIEL SYSTEMS ANALYSIS ACTIVITY P DIETZ 392 HOPKINS RD AMXSY TD APG MD 21005-5071
1	DIRECTOR US ARMY RESEARCH LAB AMSRL OP AP L APG MD 21005-5066
90	DIR USARL AMSRL CI AMSRL CI S A MARK AMSRL CS IO FI M ADAMSON AMSRL SL BA AMSRL SL BL D BELY R HENRY AMSRL SL BG AMSRL SL I AMSRL WM J SMITH AMSRL WM B A HORST AMSRL WM BA D LYON AMSRL WM BC P PLOSTINS J NEWILL S WILKERSON A ZIELINSKI AMSRL WM BD B FORCH R FIFER R PESCE RODRIGUEZ B RICE AMSRL WM BE C LEVERITT AMSRL WM BF J LACETERA AMSRL WM BR C SHOEMAKER J BORNSTEIN

NO. OF COPIES ORGANIZATION

ABERDEEN PROVING GROUND (CONT)

AMSRL WM M
D VIECHNICKI
G HAGNAUER
J MCCAULEY
AMSRL WM MA
L GHIORSE
S MCKNIGHT
AMSRL WM MB
B FINK
J BENDER
T BOGETTI
R BOSSOLI
L BURTON
K BOYD
S CORNELISON
P DEHMER
R DOOLEY
W DRYSDALE
G GAZONAS
S GHIORSE
D GRANVILLE
D HOPKINS
C HOPPEL
D HENRY
R KASTE
M KLUSEWITZ
M LEADORE
R LIEB
E RIGAS
J SANDS
D SPAGNUOLO
W SPURGEON
J TZENG
E WETZEL
A FRYDMAN
AMRSL WM MC
J BEATTY
E CHIN
J MONTGOMERY
A WERECZCAK
J LASALVIA
J WELLS
AMSRL WM MD
W ROY
S WALSH
AMSRL WM T
B BURNS
M ZOLTOSKI

NO. OF COPIES ORGANIZATION

ABERDEEN PROVING GROUND (CONT)

AMSRL WM TA
W GILLICH
T HAVEL
J RUNYEON
M BURKINS
E HORWATH
B GOOCH
W BRUCHEY
M NORMANDIA
AMRSL WM TB
D KOOKER
P BAKER
AMSRL WM TC
R COATES
AMSRL WM TD
A DAS GUPTA
T HADUCH
T MOYNIHAN
F GREGORY
M RAFTENBERG
M BOTELER
T WEERASOORIYA
D DANDEKAR
A DIETRICH
AMSRL WM TE
A NIILER
J POWELL
AMSRL SS SD
H WALLACE
AMSRL SS SE DS
R REYZER
R ATKINSON

NO. OF COPIES	ORGANIZATION
1	LTD R MARTIN MERL TAMWORTH RD HERTFORD SG13 7DG UK
1	SMC SCOTLAND P W LAY DERA ROSYTH ROSYTH ROYAL DOCKYARD DUNFERMLINE FIFE KY 11 2XR UK
1	CIVIL AVIATION ADMINSTRATION T GOTTESMAN PO BOX 8 BEN GURION INTERNL AIRPORT LOD 70150 ISRAEL
1	AEROSPATIALE S ANDRE A BTE CC RTE MD132 316 ROUTE DE BAYONNE TOULOUSE 31060 FRANCE
1	DRA FORT HALSTEAD P N JONES SEVEN OAKS KENT TN 147BP UK
1	DEFENSE RESEARCH ESTAB VALCARTIER F LESAGE COURCELETTE QUEBEC COA IRO CANADA
1	SWISS FEDERAL ARMAMENTS WKS W LANZ ALLMENDSTRASSE 86 3602 THUN SWITZERLAND

NO. OF COPIES	ORGANIZATION
1	DYNAMEC RESEARCH AB AKE PERSSON BOX 201 SE 151 23 SODERTALJE SWEDEN
1	ISRAEL INST OF TECHNOLOGY S BODNER FACULTY OF MECHANICAL ENGR HAIFA 3200 ISRAEL
1	DSTO WEAPONS SYSTEMS DIVISION N BURMAN RLLWS SALISBURY SOUTH AUSTRALIA 5108 AUSTRALIA
1	ECOLE ROYAL MILITAIRE E CELENS AVE DE LA RENAISSANCE 30 1040 BRUXELLE BELGIQUE
1	DEF RES ESTABLISHMENT VALCARTIER A DUPUIS 2459 BOULEVARD PIE XI NORTH VALCARTIER QUEBEC CANADA PO BOX 8800 COURCELETTE GOA IRO QUEBEC CANADA
1	INSTITUT FRANCO ALLEMAND DE RECHERCHES DE SAINT LOUIS DE M GIRAUD 5 RUE DU GENERAL CASSAGNOU BOITE POSTALE 34 F 68301 SAINT LOUIS CEDEX FRANCE
1	ECOLE POLYTECH J MANSON DMX LTC CH 1015 LAUSANNE SWITZERLAND

NO. OF COPIES	ORGANIZATION
1	TNO DEFENSE RESEARCH R IJSSELSTEIN ACCOUNT DIRECTOR R&D ARMEE PO BOX 6006 2600 JA DELFT THE NETHERLANDS
2	FOA NATL DEFENSE RESEARCH ESTAB DIR DEPT OF WEAPONS & PROTECTION B JANZON R HOLMLIN S 172 90 STOCKHOLM SWEDEN
2	DEFENSE TECH & PROC AGENCY GROUND I CREWTHER GENERAL HERZOG HAUS 3602 THUN SWITZERLAND
1	MINISTRY OF DEFENCE RAFAEL ARMAMENT DEVELOPMENT AUTH M MAYSELESS PO BOX 2250 HAIFA 31021 ISRAEL
1	TNO DEFENSE RESEARCH I H PASMAN POSTBUS 6006 2600 JA DELFT THE NETHERLANDS
1	B HIRSCH TACHKEMONY ST 6 NETAMUA 42611 ISRAEL
1	DEUTSCHE AEROSPACE AG DYNAMICS SYSTEMS M HELD PO BOX 1340 D 86523 SCHROBENHAUSEN GERMANY

REPORT DOCUMENTATION PAGE

Form Approved
OMB No. 0704-0188

1. AGENCY USE ONLY *(Leave blank)*	2. REPORT DATE	3. REPORT TYPE AND DATES COVERED
	January 2002	Final, January 1997 – January 1998

4. TITLE AND SUBTITLE

Thermochemical Response of Vinyl-Ester Resin

5. FUNDING NUMBERS

622618.H80

6. AUTHOR(S)

Bruce K. Fink, Travis A. Bogetti, Molly A. Stone,* and John W. Gillespie, Jr.*

7. PERFORMING ORGANIZATION NAME(S) AND ADDRESS(ES)

U.S. Army Research Laboratory
ATTN: AMSRL-WM-MB
Aberdeen Proving Ground, MD 21005-5069

8. PERFORMING ORGANIZATION REPORT NUMBER

ARL-TR-2653

9. SPONSORING/MONITORING AGENCY NAMES(S) AND ADDRESS(ES)

10.SPONSORING/MONITORING AGENCY REPORT NUMBER

11. SUPPLEMENTARY NOTES

*University of Delaware, Newark, DE 19716

12a. DISTRIBUTION/AVAILABILITY STATEMENT

Approved for public release; distribution is unlimited.

12b. DISTRIBUTION CODE

13. ABSTRACT *(Maximum 200 words)*

This report presents the thermochemical characterization of Dow Derakane 411-C50 commercial vinyl-ester resin at low temperatures (20°–40 °C). Differential scanning calorimetry (DSC) and torsional braid analysis (TBA) are the experimental techniques used to characterize the material behavior. The cure kinetics are studied using DSC and are modeled using a modified autocatalytic equation with a maximum degree of cure term. Also, the effect of inhibitors in the resin system is accounted for by an inhibitor depletion model. A time-temperature-transformation diagram is constructed for the material by measuring the times to gelation and vitrification using TBA. The glass transition temperature (T_g) is also characterized using the TBA and related to the degree of cure. It was found that the T_g and the degree of cure do not exhibit a linear relationship for this resin system. The findings presented in this work provide information for accurate cure modeling and process simulation of vinyl-ester materials.

14. SUBJECT TERMS

composites, vinyl ester, torsional braid analysis, differential scanning calorimetry

15. NUMBER OF PAGES

51

16. PRICE CODE

17. SECURITY CLASSIFICATION OF REPORT	18. SECURITY CLASSIFICATION OF THIS PAGE	19. SECURITY CLASSIFICATION OF ABSTRACT	20. LIMITATION OF ABSTRACT
UNCLASSIFIED	UNCLASSIFIED	UNCLASSIFIED	UL

INTENTIONALLY LEFT BLANK.